Astron. Astrophys. 357, 850–870 (2000)

ASTRONOMY AND ASTROPHYSICS

Stellar populations in active galactic nuclei

II. Population synthesis⋆

C. Boisson[1], **M. Joly**[1], **J. Moultaka**[1], **D. Pelat**[1], **and M. Serote Roos**[2,1]

[1] DAEC, Unité associée au CNRS et à l'Université Denis Diderot, Observatoire de Paris, section de Meudon, 92195 Meudon Cedex, France
[2] Observatório Astronómico de Lisboa, Tapada da Ajuda, 1349-018 Lisboa, Portugal

Received 9 August 1999 / Accepted 27 March 2000

Abstract. The relationship of an AGN to its host galaxy is one crucial question in the study of galaxy evolution. We present a method to estimate the stellar contribution in active galactic nuclei. We perform stellar population synthesis in the central regions of a sample of 12 galaxies of different levels of activity: normal galaxies, starburst galaxies, LINERs, Seyfert 2 and Seyfert 1 galaxies. Quantification of the stellar contribution is carried out in the visible range (5000 to 8800 Å) using the equivalent widths of the absorption features throughout the spectrum. The synthesis is done by a variant of the new GPG method (Pelat, 1997). This method, contrary to previous ones, gives a unique solution.

We find quite different stellar populations for the different types of activity, which seems to be indicative of an age sequence. The starburst galaxies present the youngest populations of the sample. The Seyfert 2 nuclei and NGC 1275, a Seyfert 1 with signs of interaction and where young stellar clusters have been found, also show the contribution of a young population, less intense than in the starburst galaxies but metal rich. NGC 3516, a typical Seyfert 1, has a normal population characteristic of galaxies of the same Hubble type and finally the LINERs show the oldest populations in the sample, metal rich, with little star formation still going on.

It is found that a strong CaII triplet, even though these lines are sensitive to gravity, does not imply necessarily a stellar population dominated by supergiant stars.

Key words: galaxies: active – galaxies: stellar content – galaxies: nuclei – galaxies: Seyfert – galaxies: starburst

1. Introduction

Properties of the host galaxy of active galactic nuclei (AGN), such as mass and luminosity concentration, morphological type, metallicity and age of the stellar population are expected to influence nuclear activity. Inversely the host galaxy can be affected by the presence of the AGN.

There are essentially two models to explain the activity of galactic nuclei. One is the "standard model", where the source of energy is produced by a central engine: a massive black-hole accreting material from the central cluster of stars and gas (e.g. Rees, 1984). The second is the "starburst model" (e.g. Terlevich et al., 1992), in which the activity derives from violent star formation in a dense and high metallicity environment. Both models require a reservoir of gas and an efficient way to concentrate the gas onto small nuclear regions.

There have been recently many suggestions that star formation is enhanced in the circumnuclear regions and disks of Seyfert galaxies. Some Seyfert are known to harbour circumnuclear starbursts (e.g. Nelson et al., 1996; Hunt et al., 1997; Maiolino et al., 1995, 1997), but their large dimension does not help to prove causal relationship. Analysis of the featureless continuum in type 2 Seyfert nuclei have provided indirect evidence that part of it might be produced by a compact starburst (Cid-Fernandes & Terlevich, 1995; Heckman et al., 1995). In fact, direct evidence of the existence of compact starburst dominating the UV light has been found in a few Seyfert 2 nuclei (Heckman et al., 1997; Gonzalez Delgado et al., 1998; Storchi-Bergmann et al., 1998).

The study of the stellar populations is a critical step in the analysis of AGN continuum. In the hypothesis of a non-stellar source of activity and as a way to better understand the origin of the continuum emission, it is necessary to account for the stellar contamination, which usually dominates nearby AGN spectral energy distribution in the optical and near IR wavelengths. On the other hand, it can help to verify if the central stellar cluster can be responsible for the observed activity. Thus, whatever the origin of the nuclear activity, a full account of the stellar population in the underlying host galaxy is requested.

Another crucial question not yet solved is to know whether the stellar populations in the nuclear regions of active galaxies differ from that of non-active galaxies of the same Hubble type. Correlations between CO, far-infrared and X-ray luminosities of active galaxies may indicate that the more powerful monsters live in the more actively star-forming host galaxies (Yamada, 1994). The accelerated star formation caused by dy-

Send offprint requests to: C. Boisson

⋆ Based on observations collected at the Canadian-French-Hawaiian Telescope, Hawaii, and Observatoire de Haute Provence, France.

Correspondence to: catherine.boisson@obspm.fr

namic instabilities triggering and/or fueling the nuclear activity would translate into overabundance of giant, supergiant and super metal rich (SMR) stars (Norman & Scoville, 1988; Scoville, 1992; Williams & Perry, 1994).

Few detailed studies of the stellar populations of AGN have been published up to now, mainly because of the difficulty to extract the stellar features from spectra where are mixed the stellar component, the strong emission lines plus, possibly, additional continuum components as the so-called featureless continuum (e.g. Oliva et al., 1995; Serote Roos et al., 1996a; Heckman et al., 1997; Cid-Fernandes et al., 1998; Gonzalez Delgado et al., 1998; Maoz et al., 1998; Storchi-Bergmann et al., 1998). Moreover, most of these studies are now concerned with the search of starbursts in Seyfert 2 galaxies and LINERs.

In this paper, we present a method which is well adapted for the estimation of the stellar contamination in the active nucleus. We determine the stellar population in the nucleus and the surrounding regions of a sample of AGN of different levels of activity, i.e. Seyferts 1 and 2, LINERs and Starbursts, in order to correlate the strength of the stellar features with the general properties of each class. It is not a complete sample on a statistical meaning but it intends to give insight on the diversity of the stellar populations undergoing different classes of activity. The theoretical aspects are described in Pelat (1997) and Moultaka & Pelat (2000).

In Sects. 2 and 3 are described the galaxy sample and the stellar data base selection. The population synthesis program is reviewed in Sect. 4. The results of the population synthesis are given in Sect. 5 and some implications are discussed in Sect. 6.

2. The galaxy sample

We base our study on long slit spectroscopy, in the range 5000–8800 Å, of a sample of ten active galaxies observed at CFHT. We also present two normal galaxies which may be used as templates. The observational and reduction aspects have been discussed in a companion paper (Serote Roos et al., 1998, hereafter, Paper I). When possible, several regions have been extracted on each side of the nucleus in order to better sample the host galaxy. These spectra are presented in Paper I where we discuss their general appearance thus giving a preliminary analysis of the stellar population.

The goal is to compare the composite stellar population of AGN host galaxies of different level of activities (Seyferts 1 and 2, LINERs and Starbursts) and to access the radial stellar distribution as well as the stellar population of the nucleus. The sample is selected to cover different morphological types. Table 1 gives the list of the 12 galaxies of the sample for which population synthesis is applied, together with their morphological type and level of activity.

The wide spectral domain covers a number of stellar absorption features, signatures of different stellar populations, e.g. MgI λ5175, NaI D λ5896 and 8196 Å, the near-IR CaIIT and the numerous TiO and CN bands. No observations were performed in the blue range (3500–5000 Å) as in that domain, a very large number of emission lines from the AGN overlaps the stellar features. This unfortunately implies that the hot stellar population is not well sampled as the strongest signatures of hot stars are in the short wavelength domain.

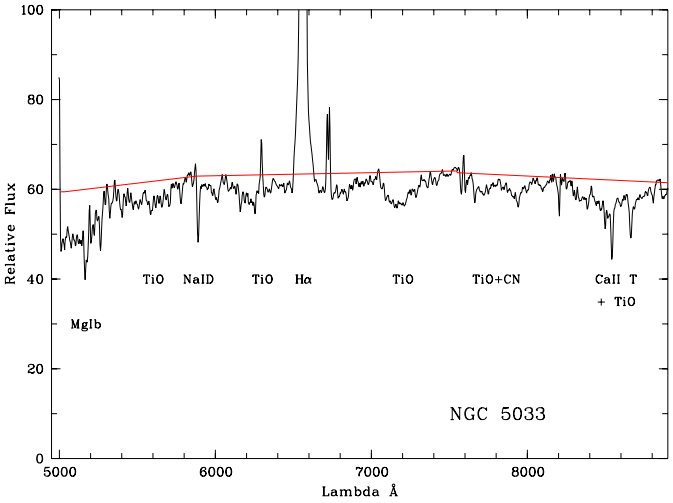

Fig. 1. Example of the continuum tracing for a typical galaxy of our sample.

In the present paper we quantify the stellar contribution to the total luminosity using the equivalent width of the absorption features whose measure is independent of the internal reddening of the galaxy.

Identification of 47 absorption lines and bands, together with the wavelength ranges used to measure the equivalent width (EW) of the features can be found in Table 2. The wavelength ranges have been defined taking into account evident differences in hot and cool star absorption features as well as the shape of these features that often are close blends of metallic lines. Although the spectral resolution would theoretically allow a finer sampling, such a sampling would decrease the signal-to-noise ratio (S/N) in each feature at the expense of the fiability of the EW measurements. As a consequence, the error-bars in the model space would increase and we would get no clearer insight on the stellar population.

The continuum level has been determined globally over the whole wavelength range. This method allows a better determination of the line strength compared to the widely used method drawing a local continuum between given pivot points which thus rely on the apparent continuum (see e.g. Bica, 1988; Cid Fernandes et al., 1998). Indeed, we want to analyse absorption features which are heavily blended and whose line ratios vary with physical conditions (e.g. TiO bands and CaIIT around 8500 Å). In such cases, the local continuum may be somewhat lower than the true integrated stellar continuum. Fig. 1 illustrates the complexity of the stellar features and shows the continuum tracing for a typical (NGC 5033) galaxy of our sample.

There are two major sources of uncertainties in the measured EW. The first one is inherent to the measurement and depends mainly on the S/N ratio. The second source of error comes from the continuum level estimation and relies somewhat on the previous one. This error is dominating over all other measurement

Table 1. Observed galaxies.

galaxy	morphology	activity level	z	σ (km s^{-1})	σ_{lit} (km s^{-1})	Ref.
NGC 1275	cD	Seyfert 1	0.018	173±46	248±17	NW
					246±18	SHI
NGC 2110	E3 or S0	Seyfert 2	0.008	192±33	220±25	NW
NGC 3310	Sbc	Starburst	0.003	112±20	111±11	TDT
NGC 3379	E3	normal	0.002	200±25	214±15	TD
					201±20	D
					209±4	BSG
NGC 3516	SB0a	Seyfert 1	0.009	144±22	235±23	TDT
					164±35	AMGB
NGC 3521	Sbc	normal	0.002	166±26	-	-
NGC 4278	E1	LINER	0.002	236±23	266±27	D
					242±13	TD
					272±27	TDT
					230±10	BSG
NGC 5033	Sc	LINER	0.003	144±16	-	-
Mrk 3	S0	Seyfert 2	0.014	193±28	248±25	TDT
					269±33	NW
Mrk 620	SBa	Seyfert 2	0.006	126±25	-	-
He 2-10	dwarf Irr	Starburt	0.002	60±20	-	-
M 81	Sb	LINER	0.	190±25	192±12	D
					174±17	TDT
					147±5	BSG
					180±14	K
					167±8	NW

AMGB: Arribas et al., 1997; BSG: Bender et al., 1994; D: Davies et al., 1987; K: Keel, 1989; SHI: Smith et al., 1990; TDT: Terlevich et al., 1990; TD: Tonry & Davis, 1981; NW: Nelson & Whittle, 1995

and statistical uncertainties. For well defined strong features (e.g. NaID, TiO, TiO+CaT) it is always less or equal to 1 Å in absolute value. It can go up to a few Å in the very blue end of the spectra as here the shape of the continuum is more rapidely changing.

Intrinsic galaxy absorption lines are velocity broadened. The velocity dispersion in the central region of each galaxy has been determined using the cross-correlation method as documented by Tonry & Davis (1979). Several parts of each spectra with clear signature of the stellar population were compared to several late type star spectra with strong absorption lines. The correlation is done in large wavelength bands free of emission lines. The procedure is carefully described in Serote Roos (1996).

The velocity dispersion was found not to vary by more than 40 km s^{-1} between the nucleus and the outer regions. The mean values of the velocity dispersion over the central part of the galaxies are given in Table 1. But, for the Seyfert galaxies, whose nuclear spectrum is too contaminated by strong emission lines, the velocity dispersion was measured only in the off-nuclear regions. Published values with references are also given. The results are in good agreement; the lower values for NGC 1275 and Mrk 3 may be due to the fact that we are sampling regions excluding the nucleus (lower velocity dispersion are expected outside the nucleus).

3. The stellar library

The stellar population synthesis requires a data base mapping at best the H-R diagram and which spectral resolution and wavelength range match those of the galaxy observations.

A few stellar libraries are available. However, they are usually restricted to solar abundance stars and to the luminosity classes V and III. Supergiant stars must be included if we want to test the validity of the starburst model. Super metal rich stars are also very important when synthesizing the stellar populations in the nuclear regions of galaxies, as large metallicities have been found in these regions (e.g. Pickles, 1985; Cayrel de Strobel, 1991; Munn, 1992).

We thus built a stellar library in order to cover the more thoroughly as possible spectral types, luminosity classes and metallicities. Particular effort has been made to include stars with measured metallicities.

Our stellar library includes 8.5 Å resolution observations at CFHT obtained during the course of the run dedicated to the galaxies and higher spectral resolution data, 4.3 Å, obtained at Observatoire de Haute Provence. These observations which concern mainly SMR and supergiant stars are described in Serote Roos et al. (1996b). In that paper we studied the behaviour of the main prominent features with the stellar types and luminosity classes. Stars of class I and II are merged in a single luminosity class, hereafter the supergiant class, as the observed stellar features have similar behaviours at our spectral resolution, in the

Table 2. The wavelength intervals measured

identification	$\lambda_{central}$	interval
FeI	5107	5058–5156
FeI,MgI+MgH	5198	5156–5240
FeI	5274	5240–5308
FeI	5336	5308–5356
FeI	5388	5356–5421
FeI,TiO,MgI	5488	5421–5554
CaI,FeI,TiO	5592	5554–5630
FeI,TiO	5653	5630–5676
FeI,NaI	5700	5676–5725
FeI,TiO	5775	5725–5825
FeI,TiO,CaI	5850	5825–5874
NaI	5894	5874–5914
FeI,Ti,MnI	5972	5914–6029
FeI,CaI	6070	6029–6110
FeI	6129	6110–6148
TiO,CaI	6178	6148–6208
TiO,FeI	6266	6208–6325
FeI,CaH,TiO	6350	6325–6374
FeI,CaI	6428	6374–6481
CaI,TiO	6508	6481–6535
Hα,TiO	6558	6535–6582
FeI,TiO	6602	6582–6622
TiO	6636	6622–6651
TiO,FeI	6670	6651–6690
TiO,FeI,CaI	6726	6690–6761
FeI,MgII	6778	6761–6795
TiO,CaH	6811	6795–6827
FeI,SiI	7008	6969–7048
TiO	7063	7048–7078
TiO,NiI,FeI	7109	7078–7140
TiO,VO	7359	7341–7377
FeI,VO	7406	7377–7434
FeI,VO	7458	7434–7482
FeI,VO	7511	7482–7540
TiO,OI	7780	7737–7823
TiO,CN,VO	7855	7823–7888
VO,CN,FeI,SiI	7929	7888–7970
FeI,CN	8015	7970–8060
TiO,FeI	8432	8411–8453
TiO,FeI	8472	8453–8490
CaII	8498	8490–8508
FeI,VO,TiI	8518	8508–8527
CaII	8542	8527–8557
FeI,VO,TiO	8601	8557–8645
CaII	8662	8645–8677
FeI,MgI	8723	8677–8768
FeI,MgI	8812	8768–8855

wavelength range considered. For similar reasons, G subgiants will be included in the dwarf luminosity class.

In order to cover the necessary range of spectral types, luminosity classes and metallicity, we broaden the observed sample by including one star spectrum from Fluks et al. (1994) and several star spectra published by Silva & Cornell (1992). The latter is the most complete library published at a resolution close to that of the galaxy observations and extending to the near-infrared. A few stars from this library were observed at OHP and the quality of our spectra relative to that of Silva & Cornell judged in reasonable agreement (Serote Roos et al., 1996b). Unfortunately, the spectra of Silva & Cornell are not cleaned from atmospheric absorption. In consequence, although special care was devoted to this correction in our galaxies and stars spectra, the domain of the telluric bands cannot be used for the galaxy synthesis.

The inclusion of Silva and Cornell's spectra is limiting the spectral resolution to 11 Å. The complete set of OHP and CFHT data is gaussian smoothed to that resolution.

As the galaxies have velocity dispersion which broadens the lines, it is usually not possible to compare directly the stellar equivalent width with the galactic ones. Given the galaxy velocity dispersions quoted in Table 1, the velocity broadening of the absorption lines is negligible compared to the spectral resolution. Thus no correction for velocity dispersion is needed.

Combining our stellar library and that of Silva & Cornell, 31 stars smoothly covering three luminosity classes (supergiants, giants and dwarfs) in the H-R diagram have been selected. The list is given in Table 3 with the name of the star, its spectral type and luminosity class and, when it is known, the metallicity with its reference. A dash for the metallicity means that no [Fe/H] information is available for this star and metallicity will be considered as solar in the following (it was verified that it is not a strong line star). The last column tells whether the spectrum is from our own obervations or from other source.

Ideally a large number of stars covering at the best resolution the H-R diagram as well as a large metallicity range is requested. However, we cannot include as many stars as would require a finer sampling in metallicity, gravity and/or temperature in order to prevent stellar library degeneracy (i.e. having two different stellar types but with spectral energy distribution similar enough to be indistinguishable in a mathematical sense). Degeneracy was tested in two steps. First, correlation matrices including all available stars were computed for continuum as well as EW informations. This was done on several wavelength ranges and over the whole spectrum. Second, it was verified for each of the 'uncorrelated' stars, that it was not possible to synthesize it with the remaining stars using the same program (see Sect. 4) as for the galaxy syntheses. In this way we checked that the two metal-rich K3III stars, which metallicities are different, are valid elements of the stellar base. Fig. 2 provides insight into the temperature and luminosity coverage of our sample. As can be seen on the H-R diagram, normal line and strong line G and K spectral types are equally sampled. This should help to decrease metallicity degeneracy in our study. Although we do not pretend to give the exact metallicity of each stellar component, we should be able to distinguish qualitatively metallic from solar population.

The wide spectral range, 5000–8800 Å, includes a large number of spectral lines sensitive to various stellar atmosphere parameters. The variations are generally complex so that a lot of different lines have to be considered. The NaI(λ8183, 8195) lines, for example, would help distinguish between the effect of overmetallicity rather than a dwarf dominated population (e.g.

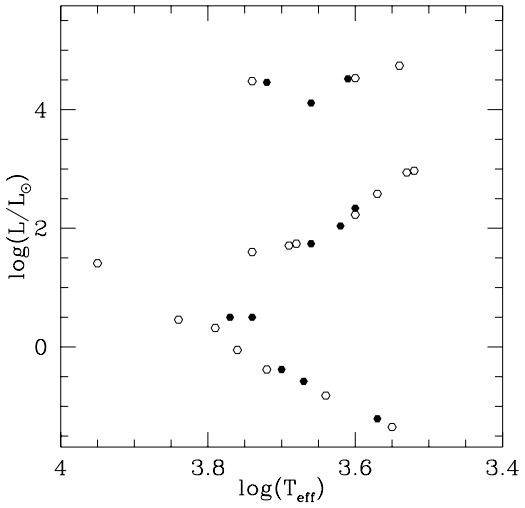

Fig. 2. H-R diagram of the stellar library. Open symbols are for solar metallicity stars; full symbols are for SMR stars. For compactness the O and B stars are not represented.

Zhou, 1991; Delisle & Hardy, 1992), but we have shown that these lines can actually be very strong in early M supergiant stars (Serote Roos et al., 1996b). The CaIIT strength is also function of several parameters: it increases with metallicity for low metallicities, i.e. half-solar and below, and saturates for metallicities higher than solar (Diaz et al. 1989). It is also a strong function of gravity and effective temperature, increasing with decreasing $T_{\rm eff}$ and $\log g$ (Diaz et al. 1989; Serote Roos et al., 1996b; Mallik, 1997). But, note that CaIIT in cool M giants or in metal rich K giants can be as strong as in normal supergiant stars. Indeed, as metallicity increases, the giant phase is cooler and both the effect of metallicity and the effect of temperature induce enhancement of the strength of the CaIIT absorption (see also Mayya, 1997). CN is a good metallicity indicator (Munn, 1992) as well as the Mg_2 index (Couture & Hardy, 1990), while FeI, MgI and TiO depend on both metallicity and effective temperature (Zhou et al., 1989; Diaz et al. 1989; Delisle & Hardy, 1992).

Hot stars (O, B and A spectral types) are not expected to contribute significantly to the EW in the wavelength range 5000–8800 Å as they do not have many signatures in this part of the spectrum. Indeed, signatures are limited to Hα usually strongly overlapped by the emission line and Paschen lines partly blended with metallic lines. Nevertheless such stars have to be included in the data base since, even if they do not contribute significantly to the EW, they affect the slope of the synthetic spectra.

An ambiguity concerning the discrimination between the presence of any hot component and internal reddening should be noted here. Indeed, the effects of a hot component is to modify the slope of the continuum of the *synthetic* spectrum: it turns bluer. On the contrary, the effect of reddening on the *observed* spectra is to make it redder. Therefore, to some extent, a stronger contribution of the hot component in the synthesis together with a stronger reddening can give as good a solution as a weaker less reddened hot component. This uncertainty is nevertheless limited as an additional continuum component (due to the hot stars) would affect the EW of the lines, whereas a high intrinsic reddening would modify the shape of the spectral energy distribution. As O stars, whatever their luminosity class and subtype, have the same colors within the spectral range it will be called O in the following as a generic name.

4. The mathematical method

The stellar population synthesis problem, as it is considered here, reduces to the finding of the numbers k_i that are the contributions of stars of type i to the luminosity at a reference wavelength $\lambda_0 = 5450$ Å using EW of the absorption features (measure which is independent of the reddening).

The search for the best combination of stars to represent the stellar content of an observed galaxy is done here with a variant of the method described in Pelat (1997). We recall below the principal ingredients of this method.

The k_is must minimize a distance D defined by:

$$D^2 = \sum_{j=1}^{n_\lambda} (W_{{\rm obs}\,j} - W_{{\rm syn}\,j})^2 P_j \,, \quad P_j \geq 0 \,; \tag{1}$$

$$W_{{\rm syn}\,j} = \frac{\sum_{i=1}^{n_\star} W_{ji} I_{ji} k_i}{\sum_{i=1}^{n_\star} I_{ji} k_i} \,. \tag{2}$$

$$\sum_{i=1}^{n_\star} k_i = 1 \,. \tag{3}$$

The $W_{{\rm obs}\,j}$ are the equivalent widths of the absorption lines measured in the galaxy and the $W_{{\rm syn}\,j}$ are the equivalent widths synthesized by mean of the stellar data base. The base is entirely defined by the equivalent widths W_{ji} and continua I_{ji} of the stars. We have a number $n_\star$ of stars in the data base and a number n_λ of equivalent widths. In this paper $n_\star = 30$ stars and $n_\lambda = 47$ lines. The P_j are weighting factors assigned to the stellar features so as to reflect the differential quality of the spectrum in the different bands for a given galaxy. When a particular absorption band is affected by emission lines or any defect, P_j is set to zero.

The physics of the problem imposes the important constraint:

$$k_i \geq 0 \,. \tag{4}$$

One of the difficulties with this system of equations, is that the k_is enter non-linearly in (1). The idea is therefore to linearize this constraint around a 'first guess'. This linearization allows a *unique* solution which is closed to the true solution of the problem for S/N$\geq$50. Details can be found in Pelat (1997).

In contrast with standard search methods we have done a change of variables which ensures that the constraints: $k_i > 0$, are *automatically* satisfied and that the coverage of the k_is is uniform (therefore no stellar population is privileged relative to an other in the search).

Table 3. The stellar base

name	spectral type	$[\frac{Fe}{H}]$	Ref.	origin
HD 44811,242935,237007	O	-		S&C
HD 37767,240344	B3-4 V	-		S&C
HD 116608,190785,124320,221741	A1-3 V	-		S&C
HD 88815	F2 V	-		CFHT
HD 187691,s65426	F8-9 V	-		S&C
HD 38858	G4 V	-		CFHT
HD 149661,151541,33278,23524,s66004,s84725	G9K0 V	0.01,0.12,0.00,0.00,0.08,-0.23	S&C	S&C
SAO 76803	K5 V	-		S&C
HD 119850	M2 V	-		S&C
HD 121370	rG0 IV	0.27	CS	OHP
HD 161797	rG5 IV	0.23	CS	OHP
HD 93800	rK0 V	0.43	BG	CFHT
HD 39715	rK3 V	0.33	BG	CFHT
HD 36395	rM1 V	0.60	CS	CFHT
HD 163993	wG8 III	-0.10	CS	OHP
HD 15866,25894,2506	G0-4 III	-		S&C
HD 72324	G9 III	0.00	CS	CFHT
HD 154733,21110	K4 III	0.00	CS	S&C
HD 141477	M0.5 III	-		OHP
-	M4 III	0.00		Fluks et al.
HD 123657	M5 III	-0.03	CS	OHP
HD 33506,112989	rG9 III	0.14	CS	S&C
HD 176670	rK3 III	0.09	T	OHP
HD 181984	rK3 III	0.39	FFBG	OHP
HD 139669	rK5 III	0.20	CS	OHP
HD 25361, SAO 21446	G0 I	0.00	FC	S&C
HD 168532	K4 I	0.00	CS	OHP
HD 206936	M2 Ia	-		OHP
HD 159181	rG2 Iab	0.14	CS	OHP
HD 180809	rK0 II	0.28	CS	OHP
HD 156283	rK3 I	0.32	CS	OHP

BG: Barbuy & Grenon, 1990; CS: Cayrel de Strobel et al., 1997; FC: Fry & Carney, 1997; FFBG: Faber et al., 1985; T: Taylor, 1991
r subscripts for SMR; w subscripts for below solar metallicity

Once the final solution has been found, we look for uncertainties due to observational errors on the galaxy equivalent widths. We neglect the errors on stellar library observables as it was shown that they have few effects on the deviation of the solution (Moultaka & Pelat, 2000).

We assume that the observational errors are Gaussian, therefore, the error region around observed equivalent widths ($W_{\rm obs}$) will be an hyper-ellipsoid that is characterized by a variance-covariance matrix. The diagonal components of this matrix are equal to σ_j^2, where σ_j are the standard deviations of the observed equivalent widths. The non diagonal terms are equal to $\rho_{ji}\sigma_j\sigma_i$, where ρ_{ji} is the correlation coefficient of two given observed equivalent widths. The problem is to deduce the error zone around the solution looking for the inverse image of the ellipsoid around $W_{\rm obs}$ by the application defined by 2. The deviation dk from the solution has to verify the constraint $\sum_{i=1}^{n_\star} dk_i = 0$ that derives from equation (3). Full account of the method is given in Moultaka & Pelat (2000).

The only constraint of the problem is the positivity of the k_is. To achieve acceptable stellar combinations, most studies have found it necessary to impose constraints which reflect known population relations (e.g. main sequence continuity, constrained lower-to-upper giant branch star number ratio...). There is an important drawback to this method since overconstrained solutions will merely reflect the constraints themselves, representing no real information about the composite population under study. Furthermore, adopted astrophysical constraints are usually predicated on current evolutionary theory which might not be appropriate in all cases (see e.g. Buzzoni, 1998). We will see that only a small number of stellar types are found to represent at best a stellar population as the S/N ratio is not infinite. Any more subtle distribution would only reflect an a priori solution. The aim is to get from the data what is in and not more in a first step. By altering the stellar base used to calculate the basic model, one can test the reality of the most significant properties of the galaxy spectra.

5. Results

Synthetic stellar population are computed for all the individual spectra extracted from the galaxy frames (see Sect. 2), using the stellar data base previously described(see Sect. 3). Spectra

Table 4. Stellar populations for the normal galaxies

stars	NGC 3379 nucleus 110 pc %	NGC 3379 ring 1 230 pc %	NGC 3379 ring 2 360 pc %	NGC 3521 central region 200 pc %	NGC 3521 Bica 160 pc %
O	0	0	0	0	0
B3-4 V	0	0	0	0	0
A1-3 V	0	0	0	0	0
F2 V	0	0	0	17±4	0
F8-9 V	8±3	19±1	11±7	0	0
G4 V	0	0	0	0	0
G9-K0 V	0	0	0	0	13±11
K5 V	0	0	0	0	24±5
M2 V	0	2±1	0	0	0
rG0 IV	0	0	7±12	0	0
rG5 IV	0	0	3±20	0	0
rK0 V	33±8	23±6	39±4	0	15±7
rK3 V	25±3	23±2	0	20±3	0
rM1 V	0	0	2±1	0	0
wG8 III	0	0	0	0	0
G0-4 III	0	0	0	0	31±10
G9 III	0	0	0	26±5	0
K4 III	27±8	27±4	32±4	0	0
M0.5 III	0	0	0	0	14±1
M4 III	2±0.2	6±0.2	6±1	2±1	0
M5 III	4±0.6	0	0	2±0.7	3±0.2
rG9 III	0	0	0	0	0
rK3 III	0	0	0	15±2	0
rK3 III	0	0	0	0	0
rK5 III	0	0	0	17±4	0
G0 I	0	0	0	0	0
K4 I	0	0	0	0	0
M2 I	0	0	0	0	0
rG2 I	0	0	0	0	0
rK0 II	0	0	0	0	0
rK3 I	0	0	0	2±4	0
D	13	11	5	7	16
E(B-V)	0.07	0.0	0.0	0.01	0.02

with a much too low S/N to enable reliable equivalent width measurements were discarded as well as those dominated by emission lines (see Paper I). The models are representative of the particular regions observed in each galaxy and do not intend to reflect the global properties of this galaxy.

Tables 4 to 8 show, for all activity classes, the stellar populations obtained for each region. The first rows give the name of the region, together with the radius for the nuclear region or the distance to the centre for the off-nuclear regions, in parsecs (assuming $H_0 = 75$ km/s/Mpc and $q_0 = 0$). The contribution of each stellar type to the luminosity at 5450 Å is listed below with its uncertainty and the two last rows display the mathematical distance D as defined in the previous section and the internal reddening, E_{B-V}. As the method is based on data independent on the reddening (the equivalent widths), it does not directly deliver this reddening. The intrinsic reddening is determined as the correction to be applied to the observed continuum to match the synthetic one. In this process the Galactic reddening law as parametrized in Howarth (1983) is used.

The distance D increases with the number of equivalent widths taken into account in the synthesis ($n_\lambda < 47$ when emission lines overlap the stellar features). Thus different D values are indicative of different quality of the synthesis only when a similar number of equivalent widths are used and so, the relative quality can only be assessed for spectra where the same features have been measured. This is generally true within one galaxy.

Figs. 3 to 14 show the synthetic spectra (black line) superimposed to the observed ones after internal reddening correction (grey line). Regions are labelled as in Paper I. Due to the inclusion of Silva & Cornell (1992) stars in the library (see Sect. 3), regions dominated by atmospheric band troughs appear as void on the synthetic spectra.

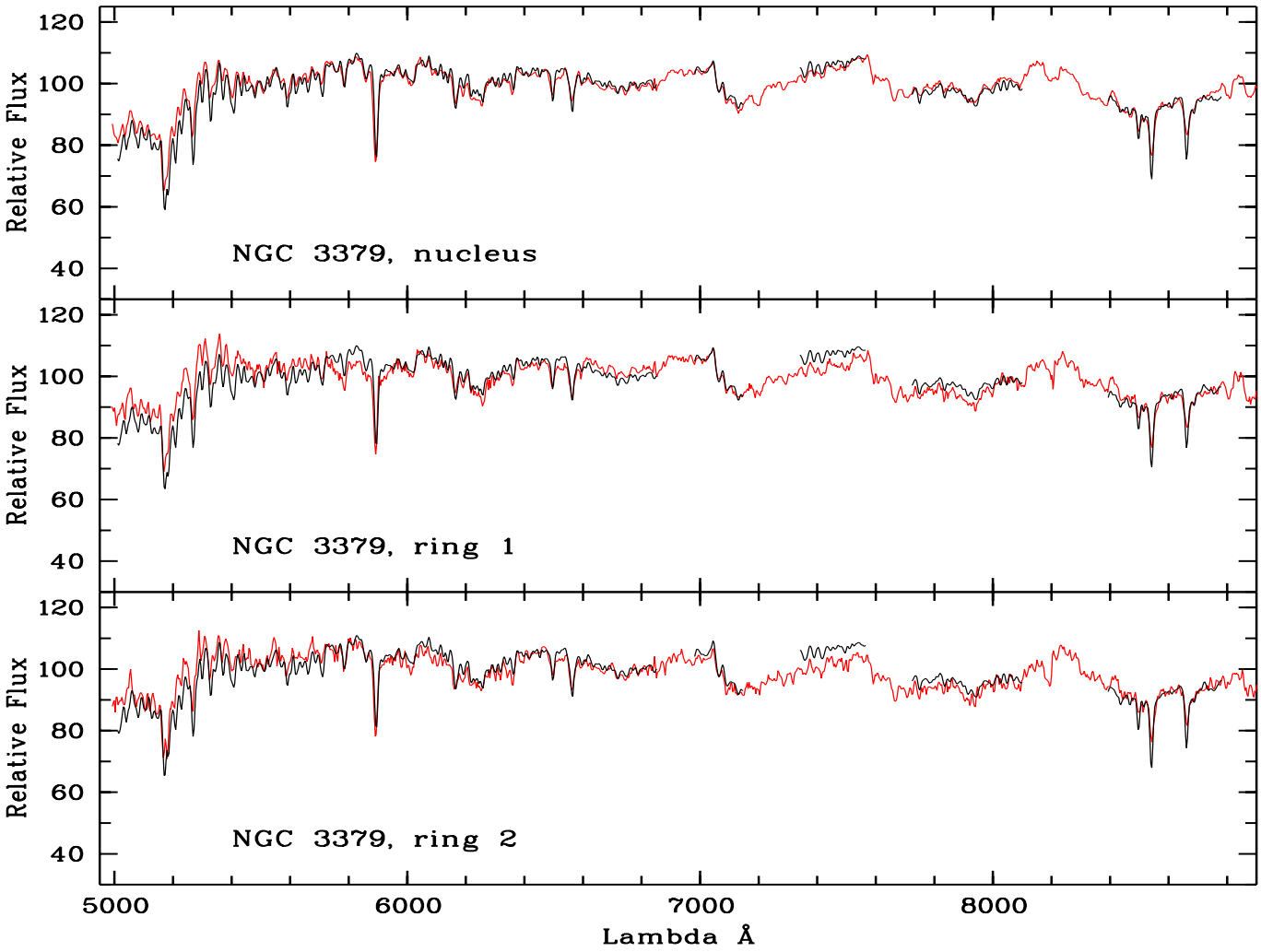

Fig. 3. The synthetic spectra (black line) superimposed to the observed ones (grey line).

5.1. The template galaxies

Our sample contains 2 template galaxies of different morphological type: NGC 3379, an elliptical, and NGC 3521, a spiral. The nucleus and 2 circumnuclear regions (rings) were synthesized for NGC 3379, whereas for NGC 3521 only a spatially averaged region of 400pc long is available. The 320 pc wide spectrum of Bica (see Bica, 1988), covering a wider wavelength range, at the requested spectral resolution of 11 Å, was also synthesized for comparison. The results of the syntheses are given in Table 4 and Figs. 3 and 4.

5.1.1. NGC 3379

The central region of the elliptical galaxy is very homogeneous in terms of population although the nucleus is found a little redder. The dominant contribution to the total radiation at λ = 5450 Å is from high metallicity dwarf stars but the evolved component is also substantial.

The observed spectral energy distribution matches the synthetic one assuming a small intrinsic reddening in the nucleus (E_{B-V}=0.07). No reddening is observed in the off-nuclear regions. The observed colour gradient (see Paper I) is due to the combination of a small dust plus a small population gradient, both gradients acting in the same direction: a redder nucleus. Small mismatch in the blue end of ring 1 is most certainly due to photometric difference between the galaxy spectrum and the stellar library flux calibrations. Indeed the distance D is very good and the error on the EW very small ($\leq$3%).

From an analysis of the far UV spectrum of the central 10 arcsec (200 pc radius) of NGC 3379, Brown et al. (1997) infer an old population of extreme horizontal branch stars (EHB) and post asymptotic giant branch stars (PAGB) of high metallicity ([Fe/H]=0.7). Our results are compatible with an old metal rich population. For the mean metallicity of the population ([Fe/H]=0.32), following Dorman et al. (1995), a turnoff around F8–9 V (1.2 $M_{\odot}$, Schmidt-Kaler, 1982) implies an age of 6–8 Gyr, somewhat younger than the age (13.8 Gyr) predicted by Bruzual & Charlot (1993) for this galaxy. However, these authors fitted the whole galaxy (120x180 arcsec) spectrum from Kennicut (1992). Indeed, Peletier et al. (1999) who studied NGC 3379 in a small (10 arcsec radius) region centered on

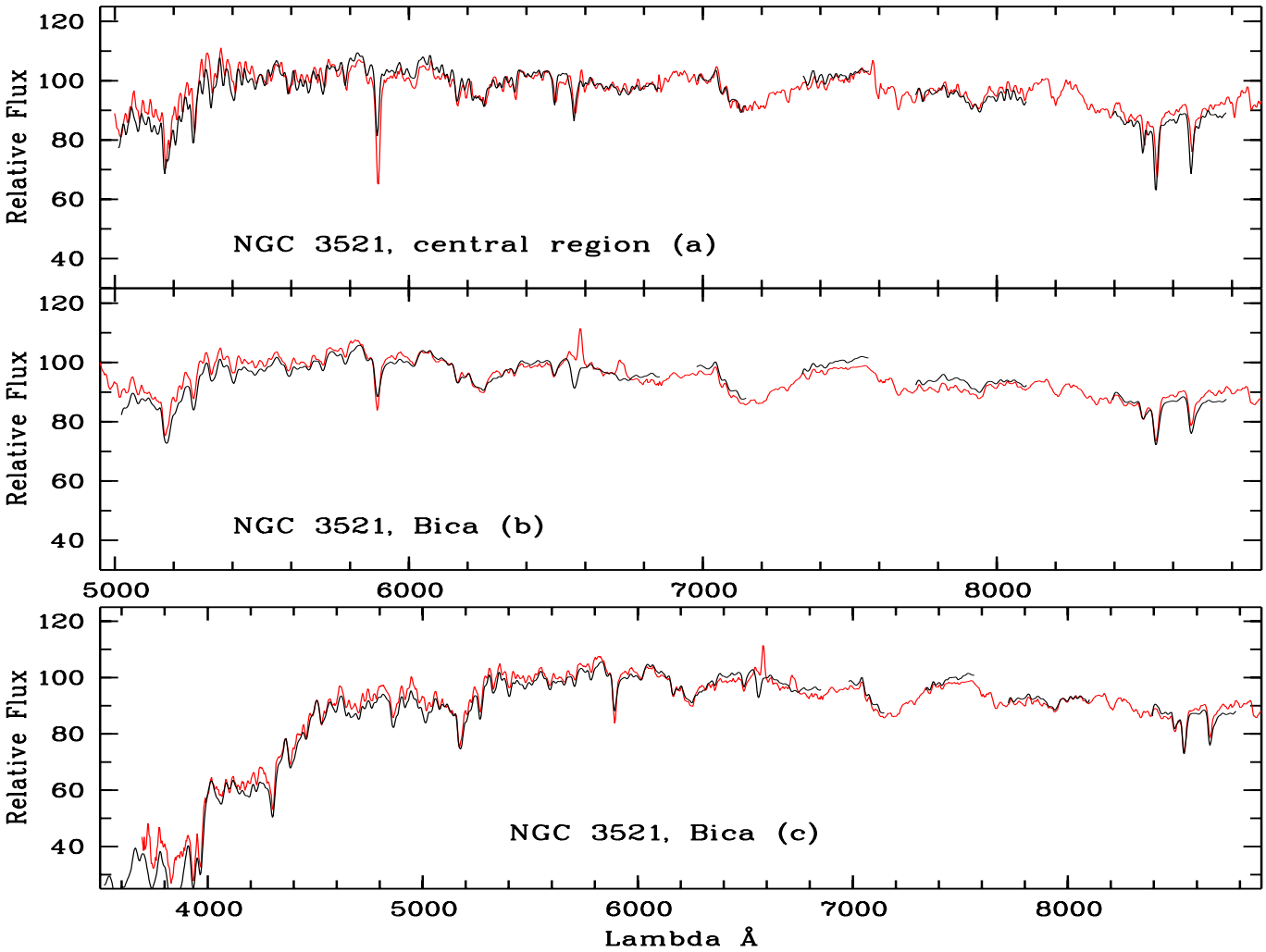

Fig. 4a–c. The synthetic spectra (black line) superimposed to the observed ones (grey line).

the nucleus find a most likely age of 8 Gyr in an homogeneous bulge stellar population.

Couture & Hardy (1993), from an analysis of the Wing-Ford band, deduce a population splitted in 55% of K dwarfs and 45% of M giants. But as stated by the authors, this very narrow range is not suited to discriminate between K dwarfs and K giants and solutions increasing the contribution of K dwarfs and giants at the expense of M giants have also been found.

5.1.2. NGC 3521

The stellar population in the central 400 pc of the spiral galaxy, NGC 3521, is somewhat younger than that of NGC 3379 with a non negligible contribution of an intermediate population, 2–4 Gyr (F2V). But the light at 5450 Å is dominated by an evolved giant component. At least half of the population is metal rich. Fig. 4a displays the synthetic spectrum (black line) superimposed on our original data after reddening correction (grey line).

The stellar population of the bulge of NGC 3521 (in a region of 5x8 arcsecond centered on the nucleus) was determined by Bica (1988). The dominant population is that of globular clusters with metallicities ranging from [Fe/H]=0.3 to -2.0. An intermediate ($\sim$1–5 Gyr) super metal rich population is found to contribute to 14% of the total light. We synthesize the spectrum published by Bica, using the information in the 5000–8800 Å domain. We find a somewhat older and less metallic population (see Table 4 and Fig. 4b). In a recent paper, Moultaka & Pelat (2000), give practical formulae to define the domain of acceptable solutions within error bars around the best solution. As an example they study the spectrum of NGC 3521 of Bica (1988). The solution published by Bica is one among many, moreover the best solution has no contribution of intermediate stars.

The difference between the stellar populations deduced from our spectrum and that of Bica's spectrum is most certainly due to the fact that the regions sampled are not exactly the same: 5x8 arcsecond for Bica and 1.2x10 for us.

Actually Bica's observation cover the wavelength range 3500–8800 Å. This gives us the opportunity of assessing the validity in the blue range of the results obtained in the visible/red domain. In order to build, from the same stellar population, a synthetic spectrum in the full range of Bica's observation

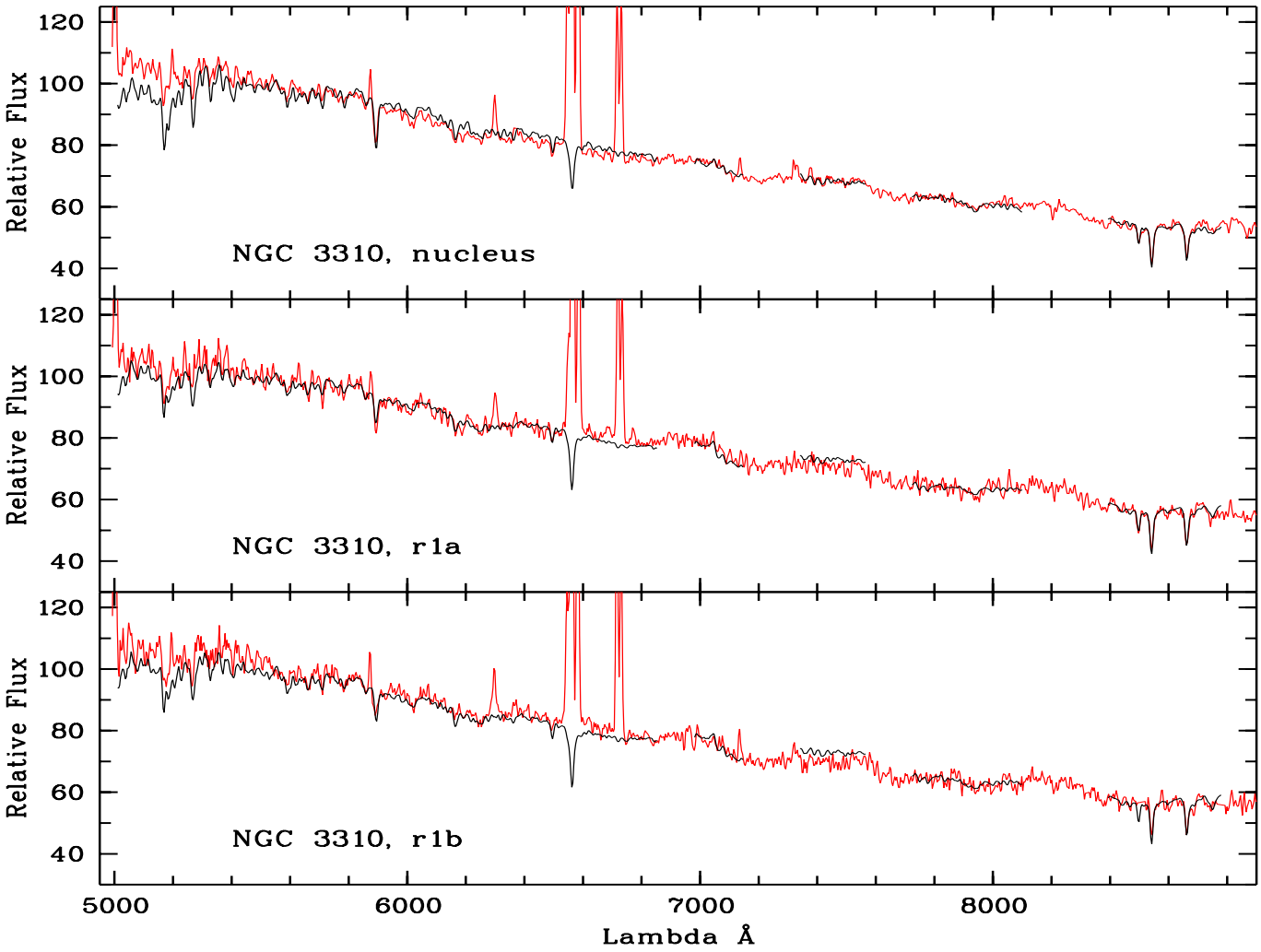

Fig. 5. The synthetic spectra (black line) superimposed to the observed ones (grey line).

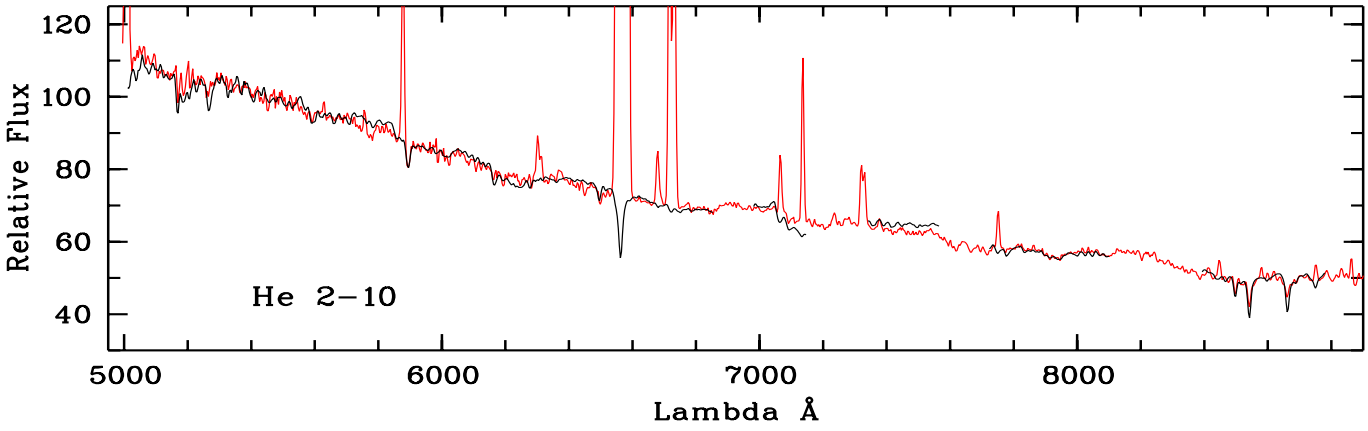

Fig. 6. The synthetic spectrum (black line) superimposed to the observed one (grey line).

(3500–8800 Å) we use only stars from Silva & Cornell's library which covers the full domain. In this library, the spectral types and luminosity classes of our library are well matched but not the metallicity. However we can check that the general shape of the synthetic spectrum is the correct one over the full wavelength range, even though the detailed of the line strength might not be perfect. The result is shown in Fig. 4c where it can be seen that the synthetic spectrum is in very good agreement with the one observed by Bica.

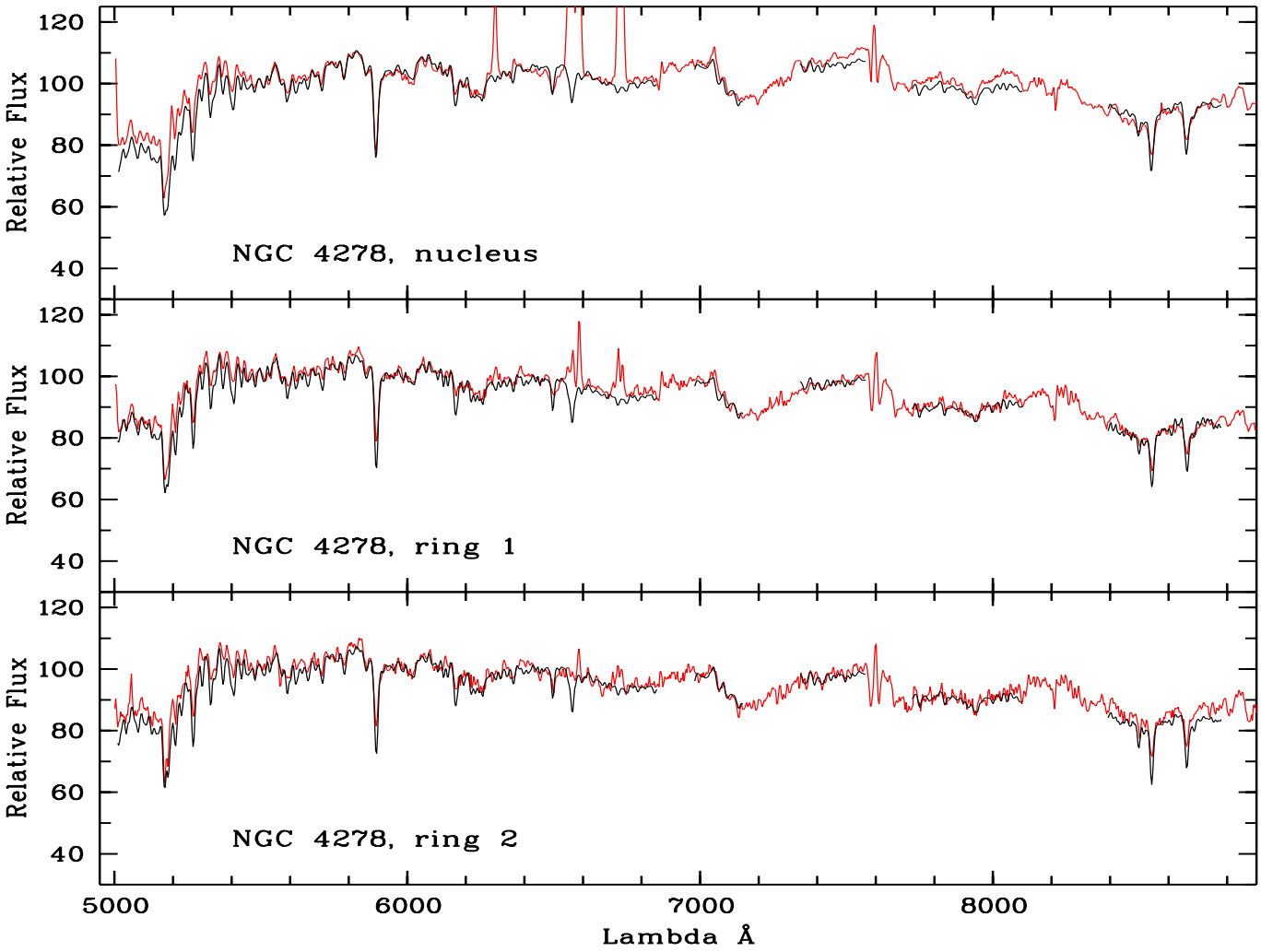

Fig. 7. The synthetic spectra (black line) superimposed to the observed ones (grey line).

5.2. The starburst galaxies

Of the two starburst galaxies, NGC 3310 is a late spiral galaxy, for which we synthesized the nucleus and two off-nucleus regions at a distance of about 350 pc from the nucleus, and He 2-10 a dwarf irregular, for which we only have a spectrum of the nucleus (Table 5).

5.2.1. NGC 3310

From the detailed study by Pastoriza et al. (1993), it can be seen that the position of the 3 regions synthesized in NGC 3310 are located on the blue compact nucleus, on the ring of Hα gas (region 1a) and in the "hole" of much lower Hα emission (region 1b). As can be seen in Table 5 a gradient of population is present in the inner bulge of NGC 3310 (i.e. within $\sim$ 1kpc in diameter). The results of the syntheses are compatible with a starburst in the nucleus and in region 1a (young stars in the nucleus; supergiants in region 1a). If the presence of O stars was confirmed in the nucleus, with no significant contribution of supergiants, it would imply a burst of star formation that occured less than 10^7 years ago (Schaerer et al., 1996). Region 1b is dominated by intermediate stars that is by an older starburst ($\sim$ 1 Gyrs) than for the other 2 regions. The synthetic spectra are shown in Fig. 5. The mismatch between the observed nuclear spectrum and the synthetic one in the extreme blue part might be linked to the large uncertainty on the O star contribution, a weak contribution of blue stars being not easily detected in the visible range.

The contribution of SMR stars is important in the nucleus which is not the case for the 2 off-nucleus regions. We checked that the presence of SMR stars is not due to artificial dilution by the hot component. Indeed, when a restricted library excluding all SMR stars is used, the mathematical distance D is considerably increased (17) and the match to the observed spectrum is far from satisfactory, implying that such a solution is not workable. A dust gradient is observed, the internal reddening vanishing outwards. The high nuclear reddening, E(B-V)=0.23, is in agreement with the value deduced from the emission line spectrum by Pastoriza et al. (1993).

In regions 1a and 1b the gas enrichment might have been weaker in the past history than in the nucleus. Pastoriza et al.

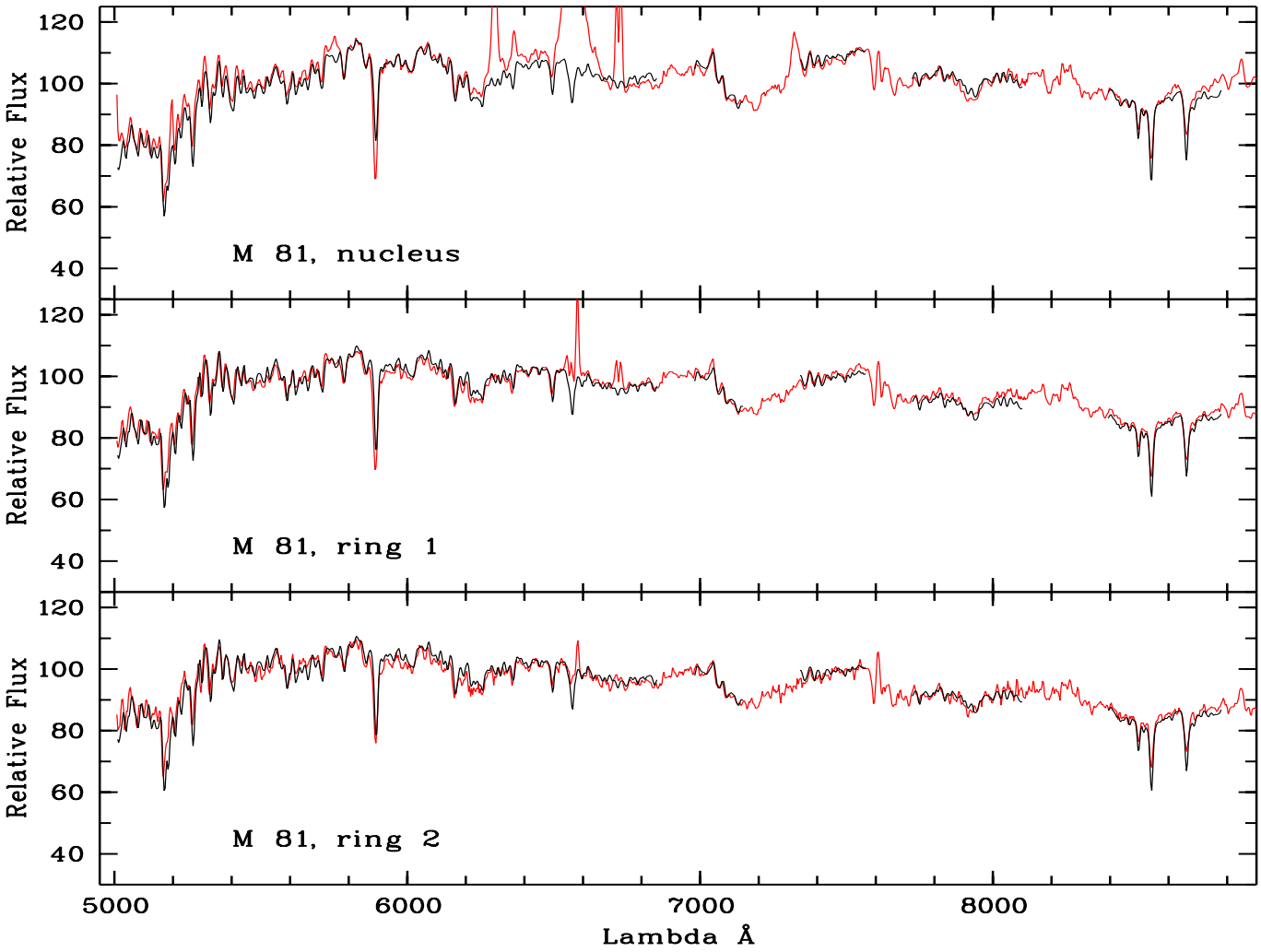

Fig. 8. The synthetic spectra (black line) superimposed to the observed ones (grey line).

propose for the circumnuclear regions two cycles of star formation. Alternatively, metal-poor gas might have been deposited in the inner regions as the result of a merger with a metal poor system (Balick & Heckman, 1981; Grothues & Schmidt-Kaler, 1991).

Assuming that the massive main sequence stars provide the bulk of the ionizing Lyman continuum photons and that case B recombination applied, the nebular lines and continuum emission produced by the hot stars can be estimated in two ways. One may estimate the number of stars from the synthesis or from the line emission intensity.

The dereddened continuum luminosity at 5450 Å is 3.6 10^{38} erg s^{-1} Å-1 and the luminosity of an O7 V star is 5.5 10^{33} erg s^{-1} $Å^{-1}$ (assuming a black-body emission of T_{eff} = 4.1 10^4 K, Vacca et al., 1996). So if O stars contribute to 4% of the observed continuum at 5450 Å, we estimate that 2600 equivalent O7 V stars are present. The nebular continuum emitted by a gas at T_e=10^4 K, n_e=100 cm^{-3}, with a helium abundance of 10% relative to hydrogen, is, taking into account HI, HII continuum radiation and two-photon decay: L_{neb}(5450 Å)=3 10^{33} erg s^{-1} $Å^{-1}$. It is only a small fraction, 2%, of the observed one.

From the dereddened Hα flux in the nucleus, we estimate an intrinsic luminosity L(Hα)=1.3 10^{40} erg s^{-1}, which corresponds to a number of ionizing photons of 2.7 10^{52} photons s^{-1}. If one assumes the production of 10^{49} photons s^{-1} for an O7 V star (e.g. Osterbrock, 1989), we deduce the presence of 950 O7 V stars following Vacca (1994) and assuming an upper mass limit of the initial mass function (IMF) of 80 $M_\odot$. This is within a factor 3 of the previous estimate. However, the latter estimation is done with a covering factor of unity which is generally not the case in nebulae. A leakage of 50% ionizing photons would enhance the number of O stars necessary to account for the lines.

5.2.2. He 2-10

This galaxy has the youngest population observed in our sample of synthesized galaxies. A strong burst of star formation seems to have occured less than 10^7 years ago. SMR stars do not contribute much, indicating a weak star formation in the

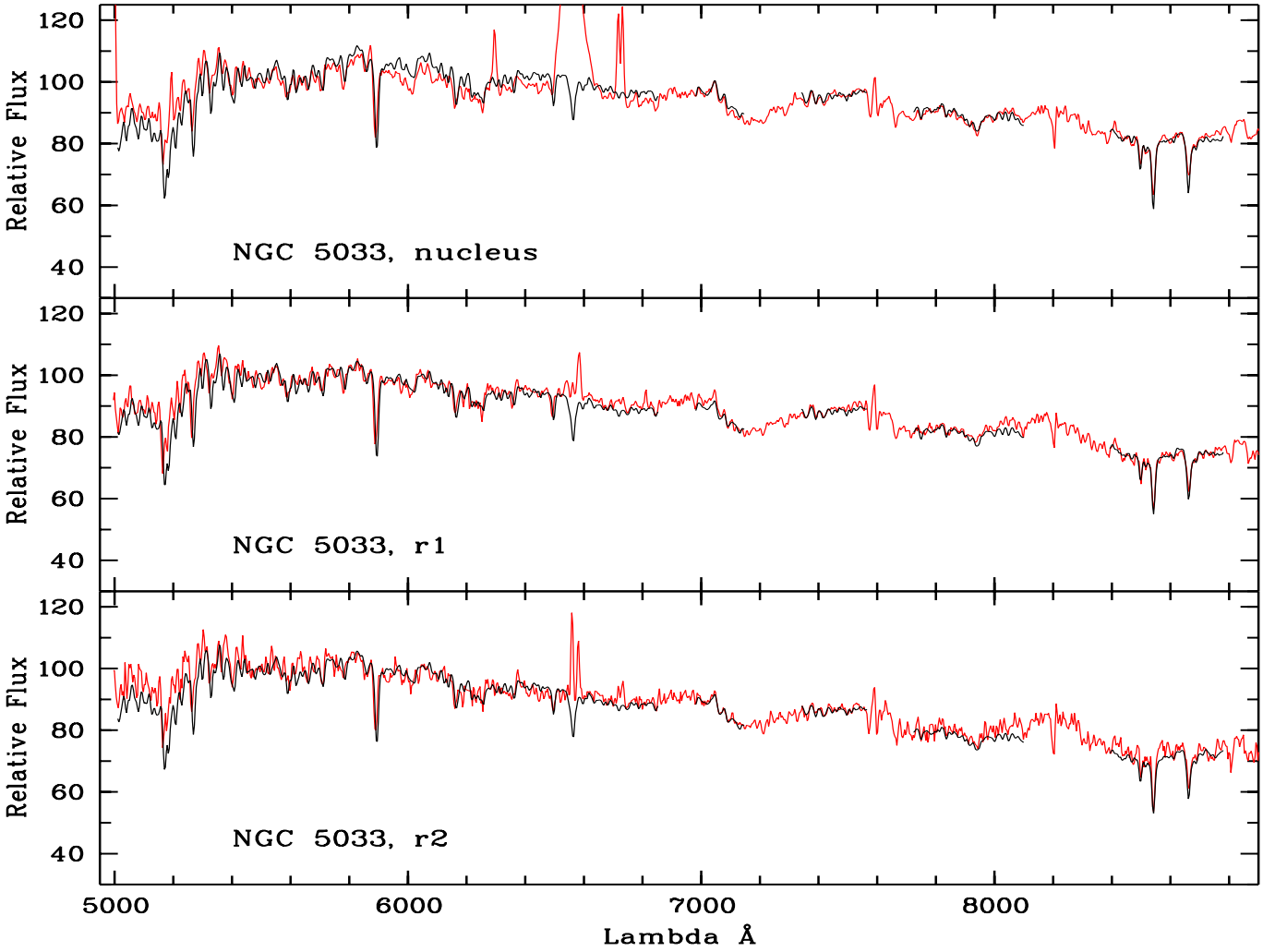

Fig. 9. The synthetic spectra (black line) superimposed to the observed ones (grey line).

past in agreement with the idea that in such galaxies the present rate of star formation is much higher than the past average one (e.g. Masegosa et al., 1994; Marconi et al., 1994; Walsh & Roy, 1993). The paucity of the metal-rich component may also indicate that recent accretion of metal-weak material contribute to this activity. We find a high contribution of hot and intermediate main sequence stars (O–F $\sim$ 80% of the radiation). The presence of Wolf Rayet stars in the spectrum (e.g. Schaerer et al., 1999) confirms recent ($\leq 10^7$ yr) star formation and the existence of massive stars. Giants and supergiants contribute no more than 10% of the total light at 5450 Å. The synthetic spectrum is shown in Fig. 6.

Our results are in agreement with Conti & Vacca (1994) who determined from HST images a very hot stellar population for He 2-10 (see also Beck et al., 1997; Schaerer et al., 1999). These authors estimate between 2500 (from the visible) and 30 000 (from the UV and IR) equivalent O stars in the central part of He 2-10. From the O stars contribution of 16% at 5450 Å in our synthesis we estimate a number of 2600 equivalent O7 V stars. The value derived from the nebular Hα line is smaller by a factor 2. But as summarized by Beck et al., a large discrepancy between all these estimations is not unexpected when the extinction is large enough that optical measurement do not see through the source (E(B-V)$_{total}\sim$0.20).

In conclusion, in spite of the difficulty underlined in Sect. 3 to evaluate the hot component, it is clear that different contribution/strength of this component can show up in our synthesis. Indeed NGC 3310 is known to have a mildly active nucleus when compared to He 2-10 as we found and Region 1a and 1b actually represent different level of activity (Fig. 1 in Pastoriza et al., 1993).

5.3. The LINERs

The LINER galaxies of the sample are the Sb and Sc galaxies M 81 and NGC 5033 respectively and the giant elliptical NGC 4278. The nuclei of all three galaxies were synthesized as well as two circumnuclear regions for M 81 and NGC 4278, whereas for NGC 5033 both synthesized regions are located north-east from the nucleus (cf. Table 6).

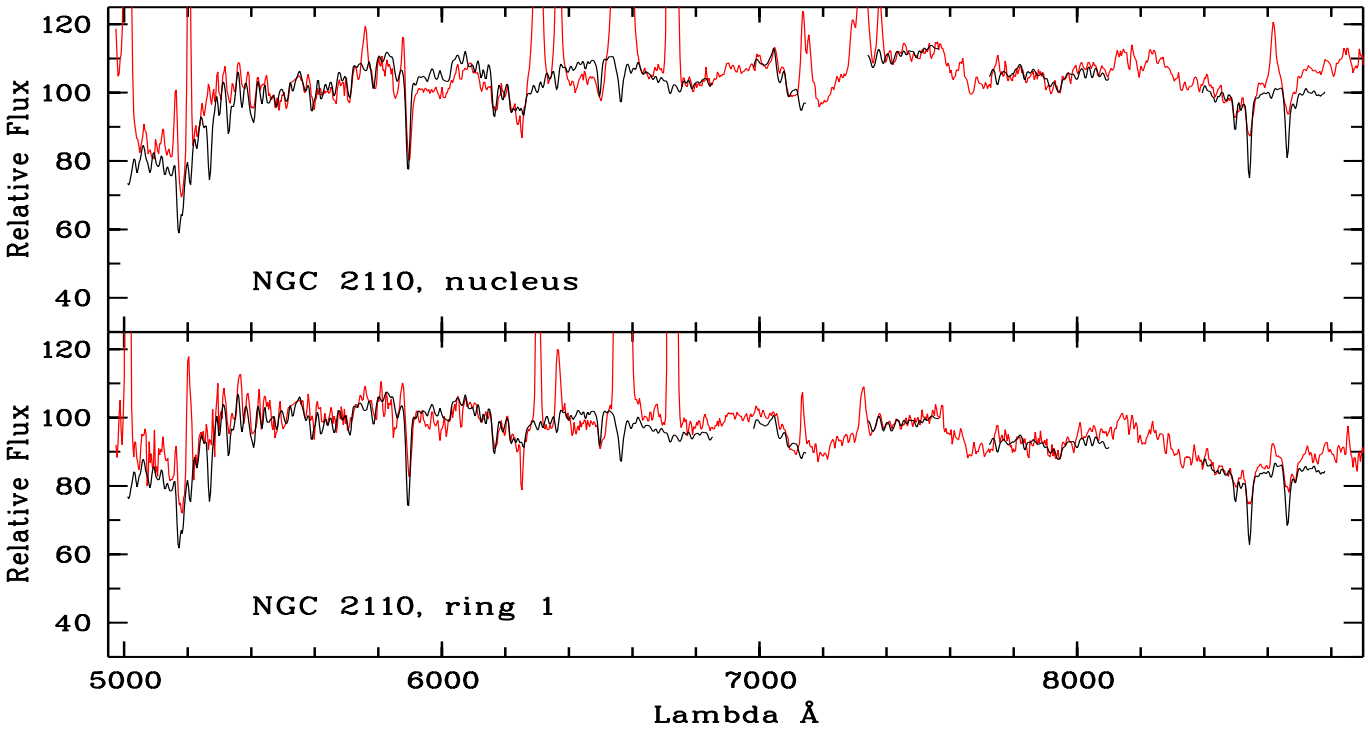

Fig. 10. The synthetic spectra (black line) superimposed to the observed ones (grey line).

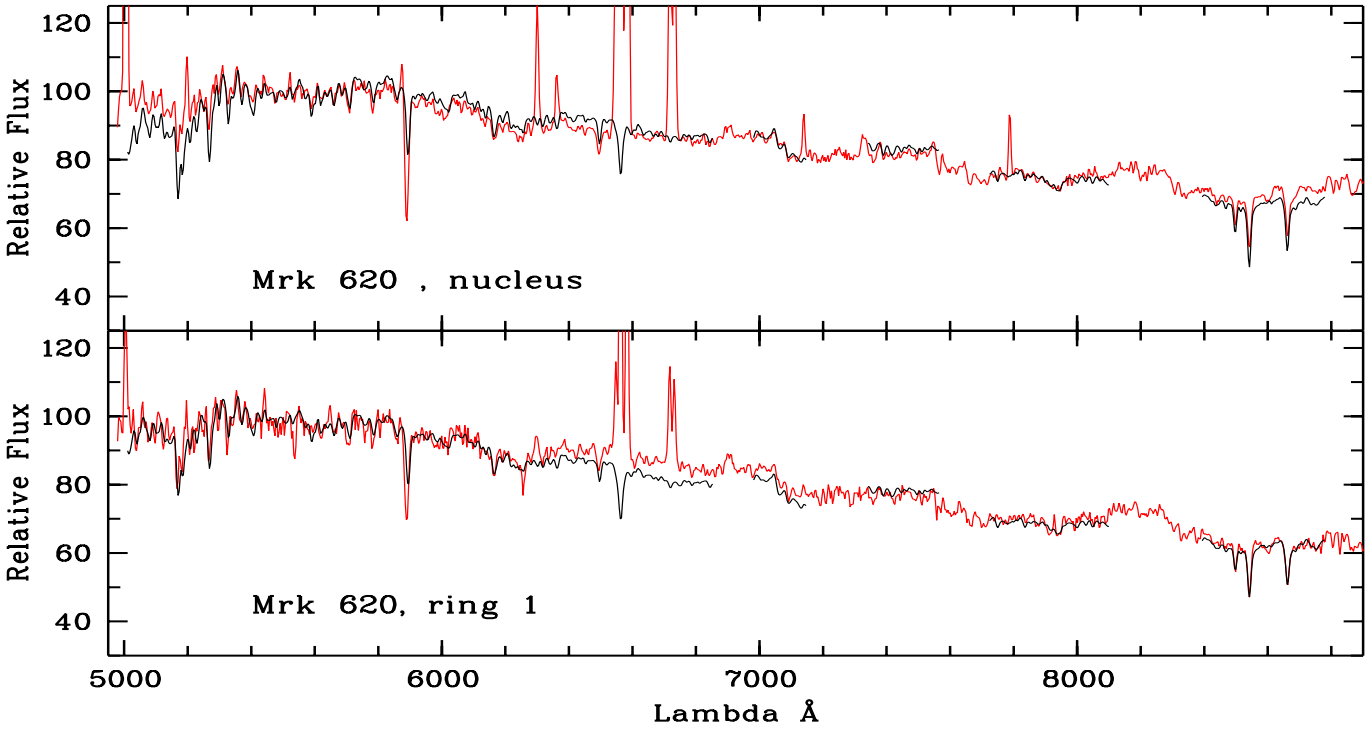

Fig. 11. The synthetic spectra (black line) superimposed to the observed ones (grey line).

5.3.1. NGC 4278

The population of the elliptical galaxy NGC 4278 is metal rich and largely dominated by late main sequence dwarfs. Evolved giant stars contribute for $\leq$20% of the total light at λ5450 Å. There is little internal reddening. The dominant population might be older than 10^9 years. In that respect NGC 4278 is similar to the elliptical galaxy NGC 3379.

However in the circumnuclear regions some younger population shows up (A and early F stars). Colour and line index gradients observed between the nucleus and circumnuclear re-

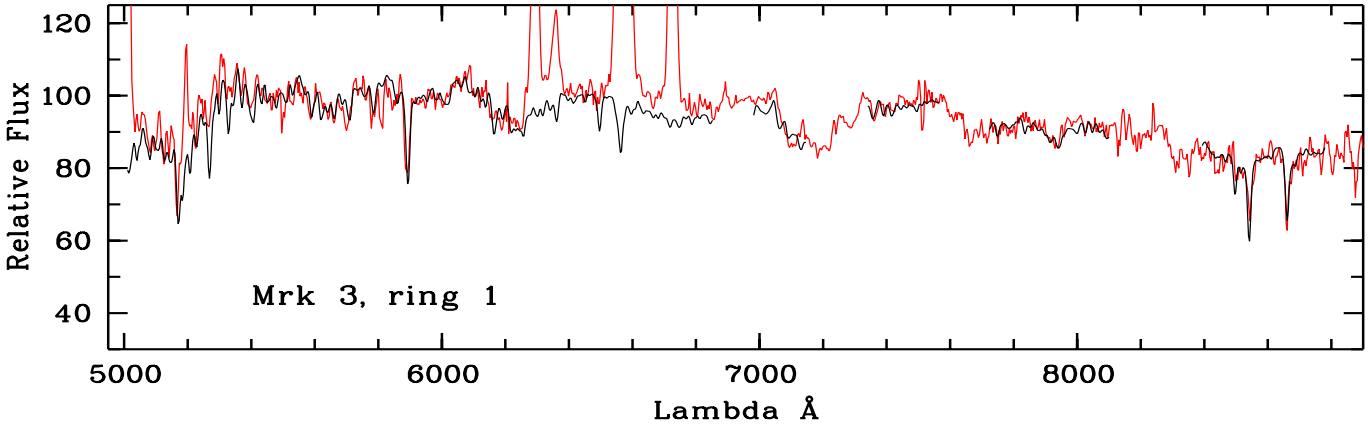

Fig. 12. The synthetic spectrum (black line) superimposed to the observed one (grey line).

gions (Møller et al., 1995; Davidge & Clark, 1994; Davies et al., 1993) can be attributed to a shallow population gradient. The synthetic spectra are shown in Fig. 7.

5.3.2. M 81

Note that the total size of the 3 regions synthesized in M 81 corresponds to the size of what is called nucleus for all other galaxies in our sample.

The population in the nucleus is more evolved than in the outer regions as the dominant contribution is from giants while late main sequence stars dominate the circumnuclear region (rings 1 and 2) as already found by e.g. Spinrad & Taylor (1971) and Faber (1972). The colour and line gradients observed in the central regions (Keel, 1989; Delisle & Hardy, 1992) are therefore due to stellar population gradients rather than dust gradient. The whole population is metal rich. The synthetic spectra are shown in Fig. 8.

Although the synthesis is made only using informations (EW and spectral energy distribution) in the visible, an estimate of the blue part of the synthetic spectrum of the nucleus is obtained using Silva & Cornell's library. This spectrum can be compared to the overall shape of the spectrum published by Ho et al. (1993) over 3500–9800 Å, in a similar aperture; see Fig. 15a for the synthetic spectrum.

5.3.3. NGC 5033

The contribution of A stars and the much higher internal reddening in all three regions of NGC 5033 indicates a somewhat younger population than in the other LINERs and in our two template galaxies. SMR stars largely dominate the stellar light. The synthetic spectra on top of the observed ones are displayed in Fig. 9.

As the mathematical distance D is very similar for all three regions, the slight population gradient between the off-nuclear regions and the nucleus should be significant; the nucleus being more evolved.

Again, validity of the synthesis at short wavelength can be checked for the nucleus, by comparing the synthetic spectrum (obtained with the Silva & Cornell's library) with the published 4000 to 7000 Å spectrum by Shuder (1980); see Fig. 15b.

In conclusion, the central regions of the three LINERs are largely dominated by a red evolved population of metal rich stars. The colour gradients discussed in Paper I are actually due to weak population gradients.

We checked that no satisfactory synthesis can be found without SMR stars in all three LINERs. The distances D would be at least a factor 3 larger.

5.4. The Seyfert 2 galaxies

The nucleus and a circumnuclear region of NGC 2110 (E3/S0) and Mrk 620 (SBa) have been studied. For Mrk 3 (S0), because of the strong emission line spectrum in the nucleus, the population synthesis was only performed in a ring extracted at about 1kpc from the centre. Results are given in Table 7.

5.4.1. NGC 2110

The stellar population in the nucleus of NGC 2110 is dominated by main sequence stars mainly SMR. The evolved population is also important but of solar metallicity. Several cycles of star formation should have occured in the past and present history of the galaxy to account for the metal enrichment of the observed population and for the suspected contribution of young stars. The uncertainty on this contribution is very large, but if confirmed, a weak burst of star formation is occuring. The synthetic spectra are displayed in Fig. 10. The slight mismatch between the two spectra are mainly due to the presence of emission lines and to photometric differences between the galaxy spectrum and the stellar library flux calibrations.

A 3% contribution of O stars at 5450 Å corresponds to 2500 O7 V equivalent stars which, if taken at face value, would be responsible of half of the Hα flux observed in our slit and to a nebular continuum less than 2% of the observed one at 5450 Å.

Validity of the synthesis at short wavelength can be checked for the nucleus, by comparing the synthetic spectrum (obtained with the Silva & Cornell's library) with the published 4000 to 7000 Å spectrum of Shuder (1980); see Fig. 15c.

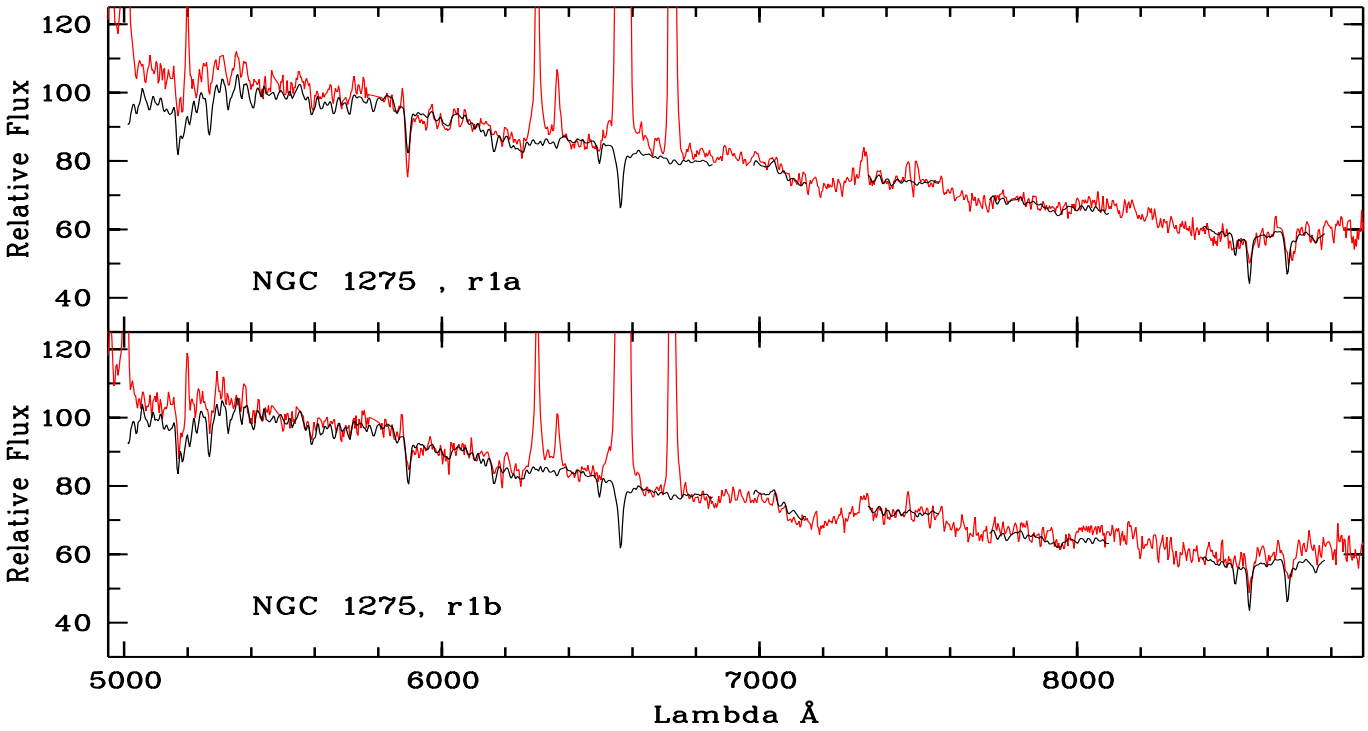

Fig. 13. The synthetic spectra (black line) superimposed to the observed ones (grey line).

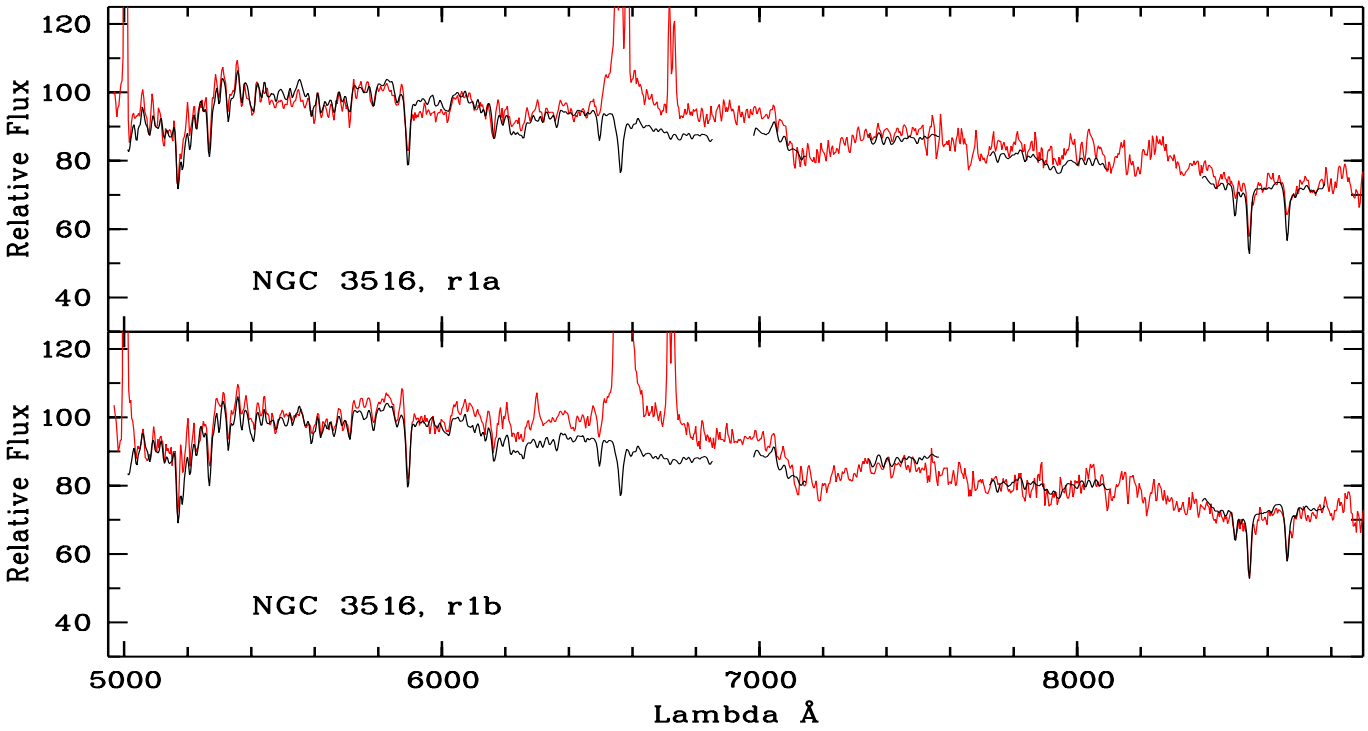

Fig. 14. The synthetic spectra (black line) superimposed to the observed ones (grey line).

In the circumnuclear region of NGC 2110 the blue component seems cooler than in the nucleus. The internal reddening is high (E_{B-V} = 0.17) and indeed, from HST imaging, important dust zones are detected offset from the nucleus (Mulchaey et al., 1994; Quillen et al., 1999). The whole population is metallic.

5.4.2. Mrk 620

Compared to NGC 2110, the stellar population of the nucleus is not as evolved: the contribution from young stars (supergiant stars) is high; giant stars contribution is low; internal reddening

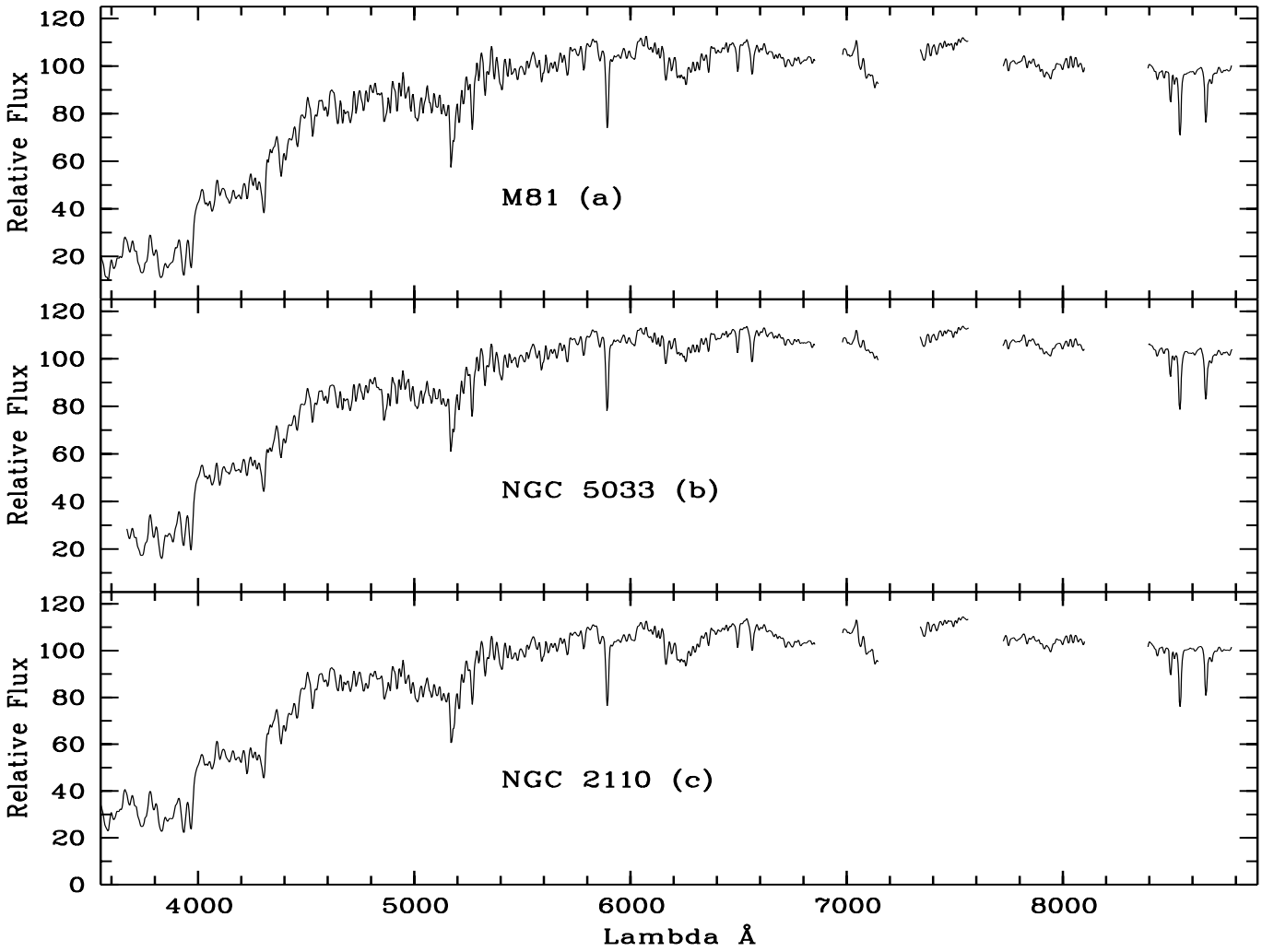

Fig. 15a–c. Synthetic spectra in the range 3500–9000 Å drawn with Silva & Cornell's stellar library.

is important. This suggests that continuous star formation in a metal rich environment is at work in Mrk 620.

In the circumnuclear region of Mrk 620 the starburst is older but the old component of the population is similar. In Fig. 11 are shown the synthetic spectra.

5.4.3. Mrk 3

The circumnuclear region of Mrk 3 is much more evolved than that of NGC 2110 and Mrk 620 but note that the region sampled is much farther (1 kpc) from the centre than the ones observed in the other two Seyfert 2 galaxies.

The synthesis shows an evolved population with some hot stars but no supergiant, no internal reddening and a large range in metallicities. See Fig. 12 for the synthetic spectra.

Although errors on the stellar contributions are small, the large distance D indicates that this galaxy spectrum is not well matched by the stellar library (a component might be missing in the library) or, more probably, that the high level of contamination by emission lines preclude reliable determination of the EW. The error on the measurements from which follows the ellipsoid error on the population may have been underestimated in this spectrum.

In conclusion, it should be noted that the metallicity of the cool star population is high in all the synthesized spectra of the Seyfert 2s. A weak recent ($\sim 2\ 10^7$ years) burst of star formation might have occured at the centre of the Seyfert 2 galaxies with an intensity decreasing with the distance to the centre or with an increasing age.

5.5. The Seyfert 1 galaxies

For both Seyfert 1 galaxies, NGC 1275 (cD) and NGC 3516 (SB0), results are only given for circumnuclear regions (Table 8) since the nuclei have very broad emission lines superimposed on the stellar spectrum.

5.5.1. NGC 1275

In NGC 1275, both off-nucleus regions are dominated by a dwarf intermediate age population (F type) of solar metallicity, which suggests the occurrence of a burst of star formation $\sim 2\ 10^9$ years

Table 5. Stellar populations for the starburst galaxies

stars	NGC 3310 nucleus 160 pc %	NGC 3310 region 1a 360 pc %	NGC 3310 region 1b 310 pc %	He2-10 nucleus 90 pc %
O	4±3	1±13	0	18±1
B3-4 V	0	0	0	0
A1-3 V	20±9	0	0	0
F2 V	0	30±13	68±3	64±2
F8-9 V	9±4	15±10	0	0
G4 V	0	12±7	0	0
G9-K0 V	0	0	0	0
K5 V	0	2±4	17±9	0
M2 V	0	0	0	1±1
rG0 IV	0	0	0	0
rG5 IV	28±11	22±6	0	8±2
rK0 V	33±5	0	12±6	0
rK3 V	0	0	0	0
rM1 V	0	0	0	2±1
wG8 III	0	0	0	0
G0-4 III	0	0	0	0
G9 III	0	0	0	0
K4 III	0	0	0	0
M0.5 III	0	0	0	2±1
M4 III	1±0.2	3±0.2	3±0.2	1±0.2
M5 III	0	0	0	1±0.3
rG9 III	0	0	0	0
rK3 III	0	0	0	0
rK3 III	0	0	0	0
rK5 III	5±2	0	0	0
G0 I	0	14±3	0	0
K4 I	0	0	0	0
M2 I	0	0	0	4±0.1
rG2 I	0	0	0	0
rK0 II	0	0	0	0
rK3 I	0	0	0	0
D	11	14	16	9
E(B-V)	0.23	0.0	0.0	0.04

ago. The suspected presence of O type stars would indicate an even younger additional component. However the error on the contribution of O stars is very large and indeed the distance D is identical for syntheses without hot component: then the contribution of F type stars is weakly enhanced. The presence of a very young starburst is thus not well established. The synthetic spectra are displayed in Fig. 13. The discrepancy in the blue ends of the spectra may partly reflect the uncertainty on the hot component but it is mainly due to the presence of emission lines.

The stellar population is quite similar to the one found in the circumnuclear regions of the starbursting galaxy NGC 3310. As mentioned in Paper I our line-of-sight intersects some of the young stellar clusters observed by Holtzman et al. (1992). It is thus reasonable to derive a population, dominated by intermediate-F stars with a possible contribution from young supergiants (~ 10 Myr).

5.5.2. NGC 3516

Serote Roos et al. (1996a) have shown that the bulge of NGC 3516 (a SB0 galaxy) is quite homogeneous with a cool stellar population which seems to be quite similar to that of the bulge of normal galaxies. In the present paper, the extent of the circumnuclear region has been defined differently: 500 pc instead of 600 pc wide. The results are somewhat different from those of Serote Roos et al. (1996a) as the mathematical method used in the present paper is much more powerful; indeed the solution previously published was a secondary minimum of the problem.

The stellar population of NGC 3516 is more evolved, but still dominated by dwarf stars, and more metal rich than that of NGC 1275. It is not much different from the bulge population of a normal galaxy. Fig. 14 shows the synthetic spectra. While the error on the contribution are small, the distance D is large in both regions. As for Mrk 3 this is due to the high level of emission line contamination. The discrepancy between the synthetic and the observed spectra around Hα/[NII] may be due to scattering from the nuclear region because of small defocusing. Results on the stellar population are not affected since no measurement is done in this region due to the continuous presence of emission lines.

Where the population is younger (region 1b), the internal reddening is higher. It is not a degeneracy problem as the solution found when the A type stars are discarded, is not acceptable: the distance D is a factor 2 larger and the shape of the synthetic spectral distribution far from the observed one.

In conclusion, the stellar population found for the two galaxies are quite different. The host galaxy of NGC 1275 is dominated by an intermediate population due to an old starburst, whereas NGC 3516 shows a population more characteristic of a normal galaxy of the same Hubble type.

6. Discussion and conclusions

In a general way, galaxies are composed of multiple populations with different ages. We find weak population and dust gradients in the central regions. The metal abundance is usually high. This metal enrichment is a direct proof of the strong star formation in the past.

The stellar population found in most of the galaxies is dominated by main sequence stars. The contribution of the late dwarfs to the integrated spectra of galaxies is a recurrent question in the litterature. Although giant dominated populations are often obtained through a few dedicated spectral indices study, the issue is far from settled (cf Pickles, 1985; Couture & Hardy, 1993; Boroson & Thompson, 1991). Indeed, if stars with high metallicities are included in the library (as it is the case in our study) the percentage of the giant contribution to the stellar population is lowered.

With respect to the SMR component, we find that without it the solutions are not suitable (the mathematical distances are much larger). Note that solutions without SMR stars do not show preferentially supergiant stars, the new populations being distributed between giants and dwarfs. So, this component is

Table 6. Stellar populations for the LINERs

stars	NGC 4278 nucleus 130 pc %	NGC 4278 ring 1 200 pc %	NGC 4278 ring 2 330 pc %	M 81 nucleus 35 pc %	M 81 ring 1 70 pc %	M 81 ring 2 160 pc %	NGC 5033 nucleus 120 pc %	NGC 5033 region 1 210 pc %	NGC 5033 region 2 420 pc %
O	0	0	0	0	0	0	0	0	0
B3-4 V	0	0	0	0	0	0	0	0	0
A1-3 V	0	16±1	0	0	2±0.9	0	7±0.6	17±1	19±1
F2 V	0	0	13±6	0	0	0	0	0	0
F8-9 V	0	0	0	0	0	0	0	0	0
G4 V	0	0	0	0	0	0	0	0	0
G9-K0 V	0	0	0	0	0	0	0	0	0
K5 V	0	0	5±7	0	0	0	0	0	0
M2 V	0	0	0	2±3	0	0	0	0	0
rG0 IV	0	0	0	0	0	10±5	0	0	0
rG5 IV	0	0	1±9	0	0	0	0	0	0
rK0 V	38±13	9±4	33±11	44±5	56±13	54±14	51±9	41±9	46±8
rK3 V	38±8	61±2	30±4	0	14±8	10±6	8±5	25±6	16±4
rM1 V	2±2	1±2	5±3	0	0	0	4±2	0	1±2
G0-4 III	0	0	0	0	0	0	0	0	0
wG8 III	0	0	0	0	0	0	0	0	0
G9 III	0	0	0	0	0	0	0	0	0
K4 III	0	0	0	0	0	1±3	0	0	0
M0.5 III	5±2	0	1±1	11±2	0	0	0	0	0
M4 III	4±0.1	3±0.5	1±0.4	2±0.5	3±0.3	2±0.3	0	0	3±0.1
M5 III	0	1±0.6	1±0.4	1±0.5	1±0.4	2±0.3	1±0.2	3±0.1	0
rG9 III	0	0	0	0	0	0	0	0	0
rK3 III	3±6	0	0	23±6	12±5	9±4	20±5	5±4	12±4
rK3 III	0	0	0	17±5	0	0	0	0	0
rK5 III	10±4	9±1	9±2	0	12±2	12±2	8±2	9±2	4±2
G0 I	0	0	0	0	0	0	0	0	0
K4 I	0	0	0	0	0	0	0	0	0
M2 I	0	0	0	0	0	0	0	0	0
rG2 I	0	0	0	0	0	0	0	0	0
rK0 II	0	0	0	0	0	0	0	0	0
rK3 I	0	0	0	0	0	0	0	0	0
D	12	10	10	9	9	7	9	8	10
E(B-V)	0.02	0.05	0.03	0.03	0.03	0.06	0.16	0.14	0.18

unavoidable and should be included in any study of the central region of galaxies.

It is worth noticing that a strong CaII triplet does not necessarily imply a stellar population dominated by supergiant stars. In many cases strong CaIIT is well accounted for by a combination of metal rich giants and/or cool dwarfs. Most of the galaxies in our sample have none or a moderate contribution of supergiant stars. Thus, even though these lines are sensitive to low gravity, one should not automatically conclude to the existence of a population of supergiant stars when they are strong (see also Mayya, 1997).

The AGN continuum is supposed to be essentially featureless in Seyfert 1 galaxies and QSO. The most common technique for starlight subtraction is the measure of dilution by this eventual featureless continuum of the nuclear absorption lines. In paper I we mention some limitations of this method either in the case where the template is the most appropriatly chosen galaxy or when it is the underlying galaxy itself. Indeed, in several cases we find population gradients between the nucleus and the circumnuclear regions within the bulge of spiral galaxies, precluding the use of the off-nucleus spectrum as a template. The detailed knowledge of the stellar population in the central regions of active galaxies is necessary to disentangle the different contributions to the nuclear emission. This is particularly true for low-level activity galactic nuclei in which star light constitutes a substantial fraction of the light. Note that for the Seyfert 2 and LINERs nuclei for which synthesis was performed, the spectral energy distribution is fully accounted for by the stellar emission plus at most 2% nebular continuum. No extra featureless continuum is evident at the signal-to-noise ratio and wavelength range of our data.

We cannot draw any conclusion about the existence of stellar population anomalies in the active nuclei studied here, but we do observe different populations for different activity types.

Table 7. Stellar populations for the Seyfert 2 galaxies

stars	NGC 2110 nucleus 260 pc %	NGC 2110 ring 1 440 pc %	Mrk 3 ring 1 1000 pc %	Mrk 620 nucleus 230 pc %	Mrk 620 ring 1 420 pc %
O	3±7	0	0	1±8	0
B3-4 V	0	0	0	0	0
A1-3 V	0	3±3	12±3	0	14±7
F2 V	0	0	0	0	0
F8-9 V	0	0	0	0	15±11
G4 V	0	0	0	21±8	0
G9-K0 V	0	0	0	0	0
K5 V	9±8	0	0	0	0
M2 V	6±2	0	0	0	0
rG0 IV	0	19±4	0	0	0
rG5 IV	9±12	0	0	19±3	32±3
rK0 V	19±6	20±7	39±6	35±4	24±4
rK3 V	22±5	36±3	6±3	0	7±3
rM1 V	0	2±0.8	0	0	0
G0-4 III	0	0	0	0	0
wG8 III	0	0	14±5	0	0
G9 III	0	0	0	0	0
K4 III	15±5	0	0	0	0
M0.5 III	12±3	0	0	1±0.6	0
M4 III	2±0.3	0	0	3±0.3	4±0.2
M5 III	0	2±0.1	2±0.1	0	0
rG9 III	0	0	0	0	0
rK3 III	0	0	0	0	0
rK3 III	0	0	0	0	0
rK5 III	3±7	18±3	27±3	0	1±0.8
G0 I	0	0	0	9±5	3±3
K4 I	0	0	0	0	0
M2 I	0	0	0	0	0
rG2 I	0	0	0	0	0
rK0 II	0	0	0	0	0
rK3 I	0	0	0	11±2	0
D	13	5	22	7	8
E(B-V)	0.05	0.17	0.05	0.20	0.10

Table 8. Stellar populations for the Seyfert 1 galaxies

stars	NGC 1275 region 1a 1100 pc %	NGC 1275 region 1b 1100 pc %	NGC 3516 region 1a 500 pc %	NGC 3516 region 1b 500 pc %
O	2±12	1±15	0	0
B3-4 V	0	0	0	0
A1-3 V	0	0	0	10±3
F2 V	47±13	65±18	37±3	0
F8-9 V	0	0	0	0
G4 V	0	0	0	24±12
G9-K0 V	0	0	0	0
K5 V	4±5	0	0	0
M2 V	0	0	0	0
rG0 IV	0	0	0	6±8
rG5 IV	24±6	0	0	0
rK0 V	0	14±7	33±5	28±4
rK3 V	9±2	11±4	0	10±4
rM1 V	0	0	5±3	0
G0-4 III	0	0	0	0
wG8 III	0	0	0	0
G9 III	0	0	0	0
K4 III	0	0	0	0
M0.5 III	0	3±1	0	0
M4 III	1±0.1	2±0.1	0	0
M5 III	0	0	1±0.3	3±0.1
rG9 III	0	0	0	0
rK3 III	4±2	0	10±7	12±5
rK3 III	0	0	0	0
rK5 III	9±2	1±3	14±3	7±1
G0 I	0	0	0	0
K4 I	0	0	0	0
M2 I	1±2	2±3	0	0
rG2 I	0	0	0	0
rK0 II	0	0	0	0
rK3 I	0	0	0	0
D	11	12	20	19
E(B-V)	0.0	0.05	0.02	0.10

Only the starburst galaxies and the nuclei of the Seyfert 2 galaxies may have a very young stellar population, attesting the occurence of a burst of star formation in the recent past. The young population of Seyfert 2 is anyway not as strong as in the starburst galaxies. As for the LINERs, they show stellar populations well evolved with little recent star formation. Such old populations are commonly observed in normal non active galaxies. If some anomalies were nevertheless present, they are extremely difficult to observe, probably because of the low spatial resolution we get from ground based observations which do not allow for a good enough separation between the nucleus and the host galaxy. In conclusion, the different stellar populations for the different types of activity might be indicative of an age sequence.

Acknowledgements. M. Serote Roos acknowledges financial support from FCT, Portugal, under grants no. PRAXIS XXI/BD /5270/95 and BPD/9995/96. We thank M. Caillat for the writing of the MEASURE program that we used to estimate the equivalent widths. J. Moultaka acknowledges financial support from LNCSR, Lebanon.

References

Arribas S., Mediavilla E., García-Lorenzo B., del Burgo C., 1997, ApJ 490, 227
Balick B., Heckman T.M., 1981, A&A 96, 271
Barbuy B., Grenon M., 1990, In: ESO/CTIO Workshop on Bulges of Galaxies. (A92-18101 05-90), p. 83
Beck S.C., Kelly D.M., Lacy J.H., 1997, AJ 114, 585
Bica E., 1988, A&A 195, 76
Bender R., Saglia, R.P., Gerhard O.E., 1994, MNRAS 269, 785
Boroson T.A., Thompson I.B., 1991, AJ 101, 111
Brown T.M., Ferguson H.C., Davidsen A.F., Dorman B., 1997, ApJ 482, 685
Bruzual A.G., Charlot S., 1993, ApJ 405, 538
Buzzoni A., 1998, In: Cosmological Parameters and Evolution of the Universe, IAUS 183, 8

Cayrel de Strobel G., 1991, In: Giannone P., Melchiorri F., Occhionero F. (eds.) Evolutionary phenomena in the Universe. p. 27
Cayrel de Strobel G., Soubiran C., Friel E.D., Ralite N., François P., 1997, A&AS 124, 299
Cid-Fernandes R., Terlevich R., 1995, MNRAS 272, 423
Cid-Fernandes R., Storchi Bergmann T., Schmitt H.R., 1998, MNRAS 297, 579
Conti P., Vacca W., 1994, ApJ 423, 97
Couture J., Hardy E., 1990, AJ 99, 540
Couture J., Hardy E., 1993, ApJ 406, 142
Davidge T.J., Clark C.C., 1994, AJ 107, 946
Davies R.L., Sadler E.M., Peletier R.F., 1993, MNRAS 262, 650
Davies R.L., Burstein, D., Dressler A., et al., 1987, ApJS 64, 581
Delisle S., Hardy E., 1992, AJ 103, 711
Diaz A.I., Terlevich E., Terlevich R., 1989, MNRAS 239, 325
Dorman B., O'Connell R.W., Rood R.T., 1995, ApJ 442, 105
Faber S.M., 1972, A&A 20, 361
Faber S.M., Friel E.D., Burstein D., Gaskell C.M., 1985, ApJS 57, 711
Fluks M.A., Plez B., Thé P.S., et al., 1994, A&AS 105, 311
Fry A.M., Carney B.W., 1997, AJ 113, 1073
Gonzalez Delgado R.M., Heckman T.M., Leitherer C., et al., 1998, ApJ 505, 174
Grothues H.G., Schmidt-Kaler Th., 1991, A&A 242, 357
Heckman T.M., Gonzalez-Delgado R.M., Leitherer C., et al., 1997, ApJ 482, 114
Heckman T.M., Krolik J., Meurer G., et al., 1995 ApJ 452, 549
Ho L.C., Filippenko A.V., Sargent W.l.W., 1993, ApJ 417, 63
Holtzman J.A., Faber S.M., Shaya E.J., et al., 1992, AJ 103, 691
Howarth I.D., 1983, MNRAS 203, 301
Hunt L.K., Malkan M.A., Salvati M., et al., 1997, ApJS 108, 229
Keel W.C., 1989, AJ 98, 195
Kennicutt R.C. Jr., 1992, ApJS 79, 255
Maiolino R., Ruiz M., Rieke G.H., Keller L.D., 1995, ApJ 446, 561
Maiolino R., Ruiz M., Rieke G.H., Papadopoulos P., 1997, ApJ 485, 552
Mallik, S.V., 1997, A&AS 124, 359
Maoz D., Koratkar A., Shields J.C., et al., 1998, AJ 116, 55
Marconi G., Matteucci F., Tosi M., 1994, MNRAS 270, 35
Masegosa J., Moles M., Campos-Aguilar A., 1994, ApJ 420, 576
Mayya Y.D., 1997, ApJ 482, L149
Møller P., Stiavelli M., Zeilinger W.W., 1995, MNRAS 276, 979
Moultaka J., Pelat D., 2000, MNRAS in press
Mulchaey J.S., Wilson A.S., Bower G.A., et al., 1994, ApJ 433, 625
Munn J.A., 1992, ApJ 399, 444
Nelson C.H., Whittle M., 1995, ApJS 99, 67
Nelson C.H., MacKenty, J.W., Simkin S.M., Griffiths R.E., 1996, ApJ 466, 713
Norman C., Scoville N., 1988, ApJ 332, 124
Oliva E., Origlia L., Kotilainen J.K., Moorwood A.F.M., 1995, A&A 301, 550
Osterbrock D.E., 1989, Astrophysics of gaseous Nebulae and Active Galactic Nuclei. University Science Books
Pastoriza M.G., Dottori H.A., Terlevich E., Terlevich R., Diaz A.I., 1993, MNRAS 260, 177
Pelat D., 1997, MNRAS 284, 365
Peletier R.F., Vazdekis A., Arribas S., et al., 1999, MNRAS 310, 863 no.559,
Pickles A.J., 1985, ApJ 296, 340
Quillen A.C., Alonso-Herrero A., Rieke M.J., McDonald C., Falcke H., 1999, ApJ in press
Rees M., 1984, ARA&A 22, 471
Schaerer D., Contini T., Kunth D., 1999, A&A 341, 399
Schaerer D., de Koter A., Schmutz W., Maeder A., 1996, A&A 312, 475
Schmidt-Kaler Th., 1982, In: Schaifers K., Voight H.H. (eds.) Landolt-Börnstein; Stars and star clusters. Numerical data and functional relationships in science and technology. Group IV, Vol. 2b
Scoville N., 1992, Relationships between active galactic nuclei and starbursts galaxies. ASP Conf. Ser. vol. 31, 159
Serote Roos M., 1996, Ph.D. Thesis, University of Paris VII
Serote Roos M., Boisson C., Joly M., Ward M.J., 1996a, MNRAS 278, 897
Serote Roos M., Boisson C., Joly M., 1996b, A&AS 117, 93
Serote Roos M., Boisson C., Joly M., Ward M.J., 1998, MNRAS 301, 1 (Paper I)
Shuder J.M., 1980, ApJ 240, 32
Silva D., Cornell M., 1992, ApJS 81, 865
Smith E.P., Heckman T.M., Illingworth G.D., 1990, ApJ 356, 399
Spinrad H., Taylor B.J., 1971, ApJS 22, 445
Storchi-Bergmann T., Cid Fernandes R., Schmitt H.R., 1998, ApJ 501, 94
Taylor B.J., 1991, ApJS 76, 715
Terlevich E., Diaz A.I., Terlevich R., 1990, MNRAS 242, 271
Terlevich R., Tenorio-Tagle G., Franco J., Melnick J., 1992, MNRAS 255, 713
Tonry J., Davis M., 1979, AJ 84, 1511
Tonry J., Davis M., 1981, ApJ 246, 666
Vacca W.D., 1994, ApJ 421, 140
Vacca W.D., Garmany C.D., Shull J.M., 1996, ApJ 460, 914
Walsh J.R., Roy J.R., 1993, MNRAS 262, 27
Williams R.J.R., Perry J.J., 1994, MNRAS 269, 538
Yamada T., 1994, ApJ 423, L30
Zhou X., Véron-Cetty M.P., Véron P., 1989, A&A 211, L12
Zhou X., 1991, A&A 248, 367